Open-Source Python Code for Modeling of Adsorption Breakthrough Performance of Zeolites for Direct Air Capture of CO2

by

Xavier Berlage Bonelli

A Thesis Presented in Partial Fulfillment
of the Requirements for the Degree
Master of Science

Approved April 2022 by the
Graduate Supervisory Committee:

Shuguang Deng, Chair
Jean Andino
Don Seo

ARIZONA STATE UNIVERSITY

May 2022

ABSTRACT

The objective of this research is to create a python program that can describe the adsorption breakthrough performance of direct air capture of CO_2 by zeolite and other adsorbents. The purpose of creating this open-source code is because many commercial simulation software for adsorption process simulation can be extremely expensive and typically are yearly subscriptions which can be a costly expenditure for academic research labs and chemical engineers working on adsorption processes development and design. The simulation models are generated by solving the governing mass and energy transfer equations and validating the models with experimental data. The typical inputs for the adsorption process simulation include adsorption equilibrium of both CO_2 and N_2 on selected adsorbents, mass transfer coefficients information, adsorbent bed length and void fraction, and other physical and chemical properties of the adsorbent being tested. The outputs of the simulation package are the dimensionless CO_2 concentration profile as a function of dimensionless time, which is usually used for evaluating the adsorbent performance for CO_2 capture. The models created were compared to the commercial package gPROMs and they performed extremely well. The main variation between the models created and gPROMs was that the models tended to underpredict the breakpoint of experimental data and gPROMs tended to overpredict. This M.S. research is part of the major research efforts for developing an open-source adsorption process simulation package for carbon capture and conversion in Prof. Deng's group at ASU. The ultimate goal of this research program is to reduce carbon emissions and develop a sustainable solution for a future carbon-free economy.

ACKNOWLEDGMENTS

I would like to thank my thesis director Dr. Shuguang Deng. He has been a wonderful mentor to me for the past two years as an educator, PI, and thesis advisor. His incredible insight into adsorption kinetics and numerical methods has been an incredible help. I would like to thank my committee members Dr. Jean Andino and Dr. Don Seo. I really appreciate their time and input into my thesis.

I would like to thank Trevor Ciha for his support and friendship since freshman year. Without him, I would have not been able to finish my studies with my sanity. His tremendous help throughout all my research has been greatly appreciated.

I would like to thank my mentor in the lab, Dr. Mai Xu. He helped me conduct my research over the past years and his guidance has helped me grow as a researcher and as a person.

I would like to thank my parents Beth and Rich and my siblings Dom and Chay. You have all been wonderful role models for me to develop my work ethic that made it possible for me to finish this rigorous coursework. I love you all.

I would like to thank all my friends who have supported me through these past four years and made me into a better man. I would like to thank Dylan Ellis, Sean Innes, and Adam Martin. I could not ask for a better group of peers- I mean I could but I am sure I would have ended up with you guys anyway.

TABLE OF CONTENTS

Page

LIST OF TABLES vi

LIST OF FIGURES vii

LIST OF SYMBOLS ix

CHAPTER

1 INTRODUCTION 1

Background 1

Problem Statement 6

Research Objectives 7

2 MATHEMATICAL MODEL FOR SIMULATION BREAKTHROUGH 9

Adsorption Breakthrough Kinetics 9

Governing Equations of Breakthrough 13

1. Adsorption Isotherm 13

2. Adsorption Kinetics 14

3. Mass Balance 14

4. Energy Balance 15

5. Momentum Balance 16

Assumptions and Final Equations 16

Numerical Methods 18

CHAPTER Page

3 MODELS FOR EXPERIMENTAL ADSORPTION BREAKTHROUGH DATA AND PREDICTED ADSORPTION BREAKTHROUGH BEHAVIOR 22

Model I: Fitting Experimental Data 22

1. Inputs 22

2. Sigmoid Function 23

3. Curve Fitting 23

4. Outputs 23

Model II: Predicting Adsorption Breakthrough Behavior 24

1. Inputs 24

2. Discretization, Initial Conditions, and Boundary Conditions 25

3. PDE Solver 26

4 RESULTS AND DISCUSSION 28

Model I 28

1. Test Case 1 28

2. Test Case 2 30

Model II 33

1. Test Case 1 33

2. Test Case 2 35

3. Model Comparison to gPROMs 38

5 SUMMARY AND FUTURE RECOMMENDATIONS 40

Page

REFERENCES 42

APPENDIX

A MODEL I AND MODEL II CODE…… ..……...46

LIST OF TABLES

Table		Page
1.	Flue Gas Composition Based on Temperature	2
2.	Base Chemical Process Simulation Software Pricing	7
3.	Template of imported .csv file of experimental data	22
4.	Initialized Matrix Components and their size	25
5.	Case 1 Model Parameters	33
6.	Case 2 Model Parameters	35
7.	Comparison between Model I, Model II, and gPROMs	39

LIST OF FIGURES

Figure Page

1. U.S. CO2 Emissions from 1990-2019 1
2. Generalized Zeolite Shapes With Type ‘a’ Shown on the Left and Types ‘x’ and ‘y’ on the Right 3
3. Visual Comparison of Physisorption and Chemisorption 4
4. Generalized PFD of an Amine-base Scrubbing Operation in a Coal Powerplant 5
5. General Apparatus of Temperature Swing Adsorption 10
6. General Apparatus of Pressure Swing Adsorption 10
7. General Apparatus of a Breakthrough Experiment 11
8. Ideal Breakthrough Adsorption Behavior 12
9. Poor Step Size for Finite Element Method 19
10. Good Step Size for Finite Element Method 19
11. Initializing Matrix for Concentration of Size M X N Where M Is the Change in Time, N Is the Change in Distance, and Matrix Values Are Concentration of Component i 20
12. Initializing Matrix for Quantity Adsorbed of Size M X N Where M Is the Change in Time, N Is the Change in Distance, and Matrix Values Are Quantity Adsorbed of Component I 21
13. Flowchart of Model I Where Orange Blocks Are Inputs by the User, Grey Blocks Are the Code Being Executed, and Red Blocks Are the Program Outputs. 24

Figure Page

14. Flowchart of Model II Where Orange Blocks Are Inputs by the User, Grey Blocks Are the Code Being Executed, Red Blocks Are the Program Outputs, and Hexagons Are Decision Points for the Code.....27

15. Breakthrough Fitting Model for Case 1.....28

16. Breakthrough Model for Case 1 Using gPROMs.....29

17. Breakthrough Fitting Model for Case 2.....31

18. gPROMs Breakthrough Model for Case.....32

19. Breakthrough Behavior Prediction Case 1.....34

20. Breakthrough Behavior Prediction Case 2.....36

21. Model II Case 2 with Reduced Superificial Velocity by a Factor of 3.....37

LIST OF SYMBOLS

Name and Symbol	Units
Equilibrium Concnetration (q^*_i)	(kg/L)
Concnetration adsorbed (q_i)	(kg/L)
Maximum Concnetration Adsorbed (q_m)	(kg/L)
Langmuir Constant (b_i)	(1/kPa)
Equilibrium pressure (p_i)	(kPa)
Equilibrium Concnetration (q^*_i)	(kg/L)
Freundlich Constant (n)	()
Intracrystalline Diffusivity (D_c)	(m^2/s)
Equilibrium Concnetration (q^*_i)	(kg/L)
Bed Radius (r)	(m)
Mass Transfer Coefficient ($K_{p,i}$)	()
Superficial Velocity (u)	(m/s)
Bed Void Fraction (ϵ)	()
Adsorbent Paricle Radius (R^2_p)	(m)
Energy Density (û)	(J/m^3)
Axial Dispersion Constant (D)	()
Component Density (ρ)	(kg/m^3)
Enthalpy of Gas Component	(J)
Thermal Conductivity (λ_{eff})	(W/m-k)
Bed Diameter (d_h)	(m)

Name and Symbol	Units
Gas Temperature (T)	(K)
Wall Temperature (T_w)	(K)
Heat Transfer Coefficient between Wall and Gas Component ($k_{T, h-w}$)	(W/m^2-K)
Enthalpy of the Bed ($h_i^{\emptyset}$)	(J)
Heat of Adsorption of Gas Component ($H_{ad, i}$)	(J/mol)
Heat Capacity of adsorbed species ($C_{p, ad, i}$)	(J/K)
Gas Mixture Thermal Conductivity (λ)	(W/m-K)
Adsorbent Thermal Conductivity (λ_{ads})	(W/m-K)
Dynamic Viscosity (μ)	(Pa/s)
Diameter of Adsorbent (d_p)	(m)
Concentration at Specific Time and Bed Length (y_i)	(M)
Bed Pressure (P_0)	(kPa)
Universal Gas Constant (R)	(kPa*L/mol-K)
Corrected Superficial Velocity (u^*)	(m/s)
Discretized Bed Length (ΔL)	()
Discretized Time (Δt)	()
Bed Concentration (C)	(kg/L)

CHAPTER 1

INTRODUCTION

1.1 Background

CO_2 is the leading contributor to global warming, and it accounts for more than 75% of greenhouse gas emissions.[1] With ever-rising emissions of greenhouse gasses from burning fossil fuels, it is necessary to not only reduce the amount of CO_2 produced but is now necessary for humanity to become carbon negative to reverse the adverse effects that the pollution of CO_2 has caused on the environment. One way to reverse the effects caused by CO_2 is to remove it from the atmosphere by using the so-called direct air capture of CO_2. CO_2 emissions per year can be seen in Figure 1 below.

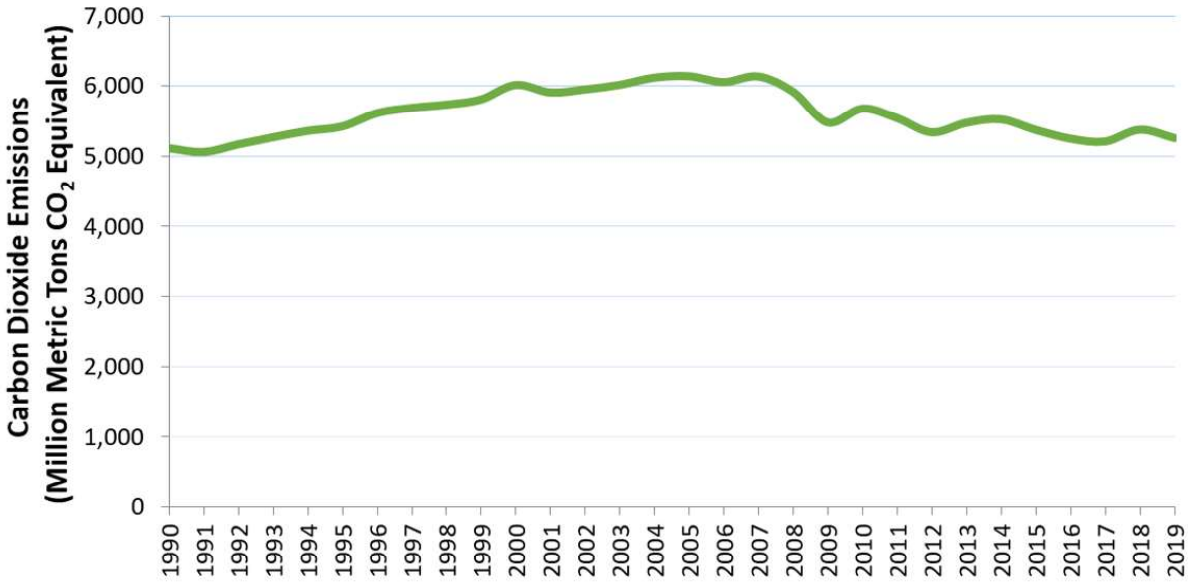

Figure 1: U.S. CO_2 Emissions from 1990-2019 [1]

The largest contributors to CO_2 emissions come from transportation, electricity, and industrial processes which account for 29%, 25%, and 23% of emissions respectively[1]. The

two main targets of CO_2 removal are flue gas and ambient air. Flue gas is the exhaust gas that is released from the combination of fossil fuels, commonly found in power plants, which contains the products of a combustion reaction.[2] It has a much higher concentration of CO_2 than ambient air. The typical flue gas composition can be seen in Table 1 below.

Table 1: Flue Gas Composition Based on Temperature[3]

Temperature (ºC)	N_2	O_2	CO_2	H_2O	SO_3 (PPM)	SO_2	NO (PPM)	OH (PPM)	CO (PPM)	H_2 (PPM)
200	76.6	2.8	14.7	5.9	1252	-	-	-	-	-
400	76.4	2.8	14.7	5.9	1239	0.001	-	-	-	-
600	76.4	2.8	14.7	5.9	787	0.04	3	-	-	-
800	76.4	2.8	14.7	5.9	152	0.11	27	-	-	-
1000	76.3	2.9	14.7	5.9	31	0.12	134	4	-	-
1200	76.3	2.9	14.7	5.9	9	0.12	425	30	3	-
1400	76.3	2.9	14.7	5.9	4	0.12	1022	144	43	5

The main problem is devising a solution that can collect the CO_2 in bulk. Ambient air is the air that is in the atmosphere and composed of approximately 79% nitrogen and 21% oxygen.[4] This type of carbon capture has the inverse problems of flue gas, meaning it has a relatively low CO_2 composition, currently the global average is about 420 PPM, so it will require a much better selectivity to achieve the same purity of CO_2 in the separation.[5,6]

Between these two targets of CO_2 capture, various techniques have been developed to remove CO_2 from the atmosphere which includes amine-based absorbents, zeolite adsorption, and caustic solution spraying. Amine-based absorbents have been proven to work well and have a high selectivity. They also work well because they can operate at flue gas conditions, however, at atmospheric pressure, their adsorption rates are significantly lower.[7,8] Amine-based solutions and other chemisorption processes will be discussed later.

Caustic solution spraying has a great advantage when it comes to a price of $53 per ton of captured CO_2, however, the drawback is that it requires compressed gas which can quickly run up prices.[9] The final technique is zeolitic adsorption, a form of physisorption. Zeolite adsorption can still work at very low pressures, atmospheric pressures, and flue gas conditions making it extremely versatile.[10,11] A large portion of its pore volume is also accessible which makes it very effective at maximizing its adsorption rate for its size.[9] Typical zeolite framework structure can be seen in Figure 2 below.

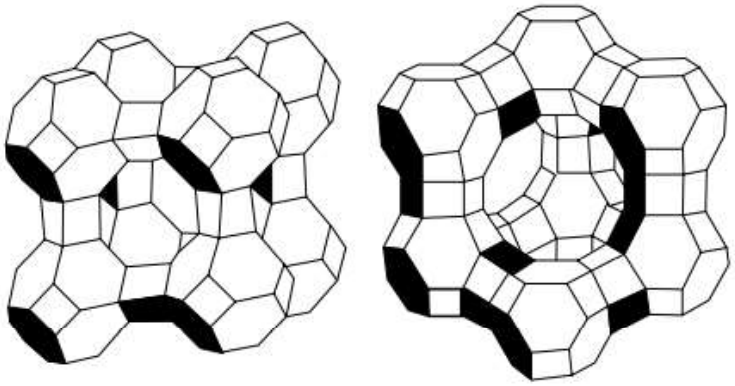

[8]*Figure 2: Generalized Zeolite Shapes with Type 'A' Shown on the Left and Types 'X' and 'Y' on the Right*

How carbon capture works with zeolite adsorption is zeolites are inserted into a packed bed and then air is fed through the column. The zeolite slurry then binds to CO_2 and allows oxygen and nitrogen to pass through. This process continues until the slurry reaches a saturation point in which it cannot trap CO_2 any further, this is known as the breakthrough point. Once the slurry has reached the breakthrough point it can no longer effectively remove CO_2 and the slurry must be replaced. The saturated slurry is then deposited underground for safe disposal. Additionally, the CO_2 can be repurposed in several other chemical processes such as the synthesis of nitrogen fertilizers, salicylic acid, and some polycarbonate plastics.[12] However, only 115 million metric tons of CO_2 are

utilized globally every year for the synthesis of various products and currently 24 billion metric tons of CO_2 are emitted yearly, thus, burying CO_2 is the primary solution.[1,12] This process can be used on regular atmospheric air in places of high pollution or directly at high CO_2 emitting sources such as factories or powerplants in the form of flue gas.[11,13]

The second major type of CO_2 removal is done via chemisorption. Chemical adsorption or chemisorption for short is the process of binding fluid components to a solid material's surface through a chemical reaction. This differs from physisorption because physisorption relies on adsorbing fluid components utilizing van der Walls forces. Whereas in chemisorption, the fluid component is bound to the surface of a sorbent with shared electrons as demonstrated in Figure 3 below.

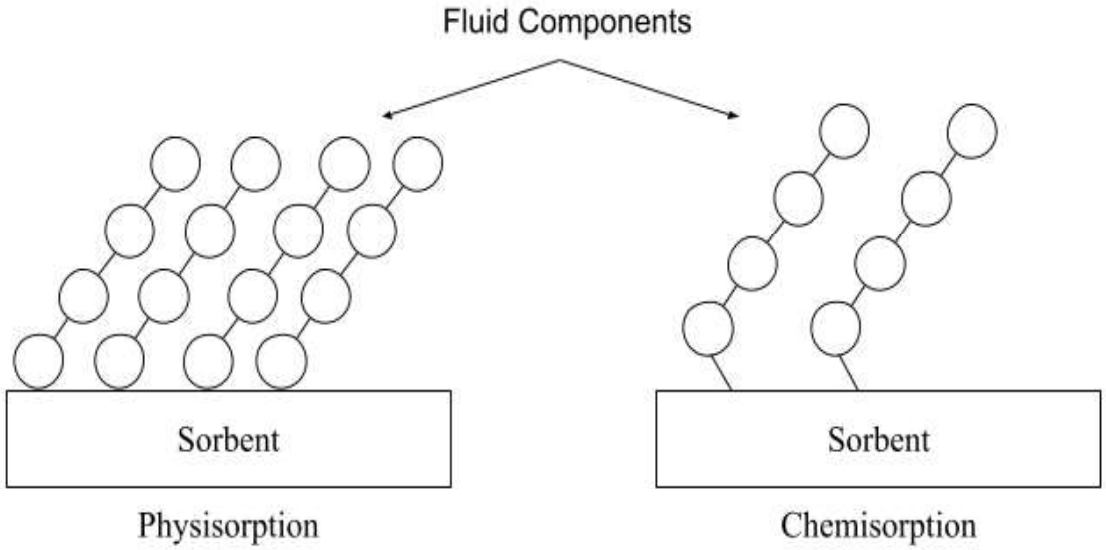

Figure 3: Visual Comparison of Physisorption and Chemisorption

As mentioned previously, a popular form of chemisorption is amine-based solutions. Amines capture CO_2 through a reversible reaction where the flue gas is fed to an adsorption unit and then goes to a desorption unit where the CO_2 is removed and stored. Amines are currently the most popular material used in the fossil fuel power plant

industry for scrubbing CO_2 in the flue gas. They require significantly less operating cost to use, which is around 3.5 GJ to capture one ton of carbon[14]. Additionally, they have a rather large capacity for carbon which is typically around 0.37 moles of CO_2 per mole of amine[15]. A typical amine scrubbing unit PFD can be seen in Figure 4 below.

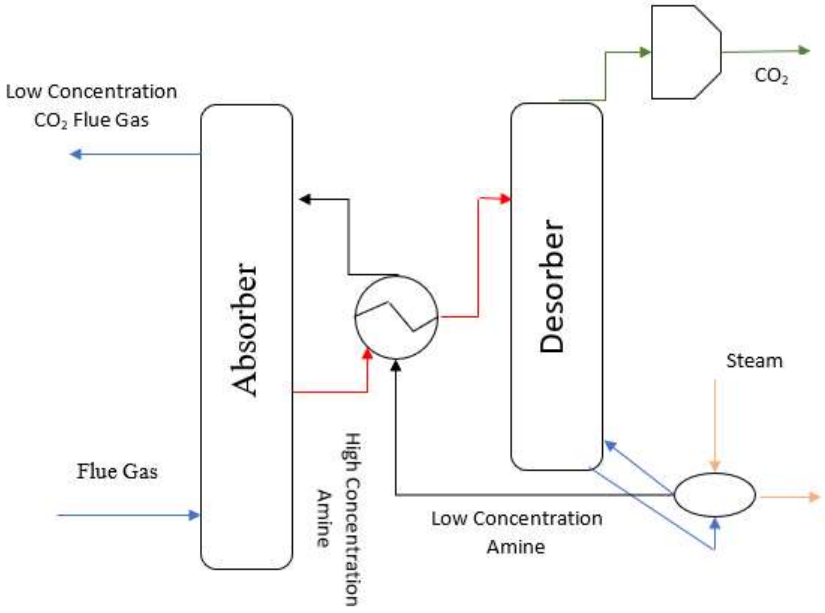

Figure 4: Generalized PFD of an Amine-base Scrubbing Operation in a Coal Powerplant

However, the major drawback of amines is that they are highly toxic and are volatile which can do more damage to the environment than help it if not properly managed. The most dangerous aspect of using amines is when they undergo degradation. Currently, many researchers have investigated the causes of degradation such as Huang et al. and their team's efforts to understand how fly ash impacts degradation[16]. Fly ash is an undesired contaminant that comes from burning coal which is found in the flue gas. Fly ash contains NO_x and SO_x compounds which act as a catalyst for degradation in monoethanolamide (MEA). The team set up a scrubbing unit loaded with MEA and tested the effects of NO_x and SO_x compounds on the activation energy for the amine to

degrade. They ran trials by pumping in a normal flue gas mixture composed of CO_2 and water vapor with and without NO_x and SO_x. What they found was that the activation energy with NO_x and SO_x dropped to 21.3 kJ/mol and without it was 152 kJ/mol. With this decrease in activation energy, degradation is significantly more favorable. It was proposed by the authors that additional unit operations should be implemented in plants to remove more of the fly ash before it reaches the scrubber to reduce the degradation kinetics. An alternative solution to the fly ash problem was proposed by Goldman et al. which uses a different type of amine: N-nitrosopiperazine (MNPZ)[17]. The benefit of this amine was that it has significantly more nitrile groups than the standard MEA and does not react as frequently when it is exposed to NO_x or SO_x. When tested under the same conditions as Huang's group, it was found that the activation energy was only 84 kJ/mol. The trade-off with using MNPZ was that it had a lower maximum adsorption capacity. However, degradation is inevitable when using aqueous amines which is why newer research is being conducted on the synthesis of amines embedded in/on solid materials.

1.2 Problem Statement

Simulation software for chemical processes is extremely expensive. Some of the most popular programs such as COMSOL, ChemCAD, Aspen Hysys, and gPROMs are thousands of dollars a year. A price breakdown of these software can be seen below in Table 2.

Table 2: Base Chemical Process Simulation Software Pricing[18]

Program	Pricing per year
COMSOL	$4,000
ChemCAD	$3,000
Aspen Hysys	$30,000
gPROMs	$2,000

While these prices are reasonable for a larger corporation, it is extremely difficult for academic research labs, and graduate and undergraduate students to procure such expensive software.

Also, many of these programs are not user-friendly; usually requiring assistance from the company itself to set up simulations. For example, in COMSOL, building and testing the basic packed bed reactor requires over 400 steps, and it does not provide error codes to the user[19.] This takes unnecessary amounts of time for communication and troubleshooting on both ends to get the program to work. Additionally, these programs are closed source. Meaning the code is not accessible from the program, so it does not allow for advanced user customization. Creating an open-source code allows free access to a customizable program that has a more directed purpose than other chemical process simulation software.

1.3 Research Objectives

This research intended to create an open-source program in Python that can produce breakthrough modeling for sorbents. The modeling of breakthroughs will enable us to

develop a process simulation package for a cyclic adsorption process (pressure swing or temperature swing adsorption processes). This was done by first taking empirical data from breakthrough experiments of sorbents and comparing those results to that of the program. Additionally, the program's model was compared to a model generated by gPROMS.

CHAPTER 2

MATHEMATICAL MODEL FOR SIMULATION BREAKTHROUGH

2.1 Adsorption Breakthrough Kinetics

Adsorption breakthrough behaviors are the measure of how a packed bed reactor (PBR) performs when adsorbing fluid components[20]. The breakthrough point is the point at which the outlet concentration of a measured component is not equal to zero. For multicomponent fluid mixture, these breakthrough points can occur at different times. A typical breakthrough experiment is set up in a PBR[21]. The bed is packed with the adsorbent and other inert materials such as silica. The bed is then degassed either by temperature swing adsorption (TSA) or pressure swing adsorption (PSA). The degassing process is used to regenerate the sorbent. The TSA process is in which the bed is heated up and treated with an inert gas like nitrogen[22]. Essentially by heating the bed, it is reversing the physisorption or chemisorption process by putting the molecules in a more excited state, so they break the bonds on the surface of the sorbent and the inert gas stream 'pushes' the released compounds out of the bed. The PSA process works like the TSA process. A vacuum is pulled on the bed and the 'pulls' the freed components out of the bed[23]. Many degassing processes will utilize both TSA and PSA to ensure that the bed has been properly purged of any foreign components to optimize the sorbents' efficiency[24]. Generalized PFDs of TSA and PSA can be seen below in Figures 5 and 6.

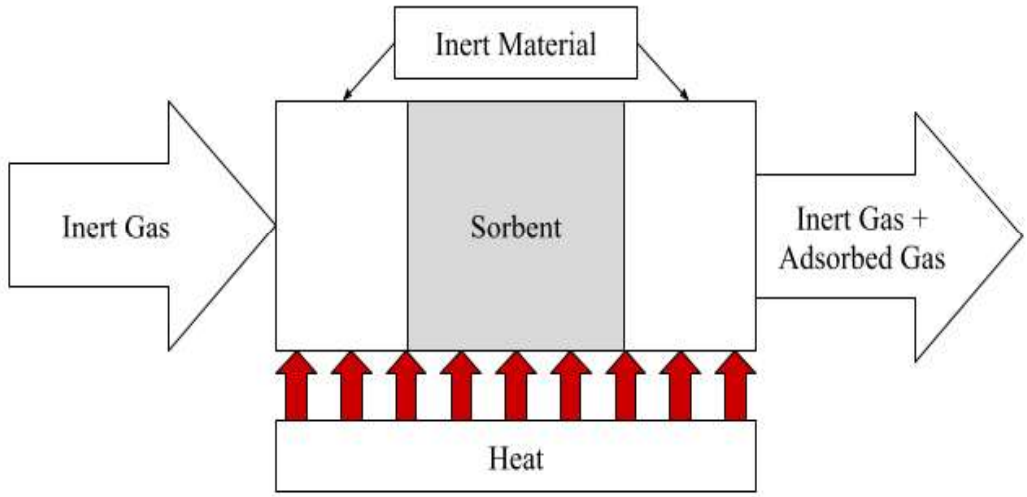

Figure 5: General Apparatus of Temperature Swing Adsorption

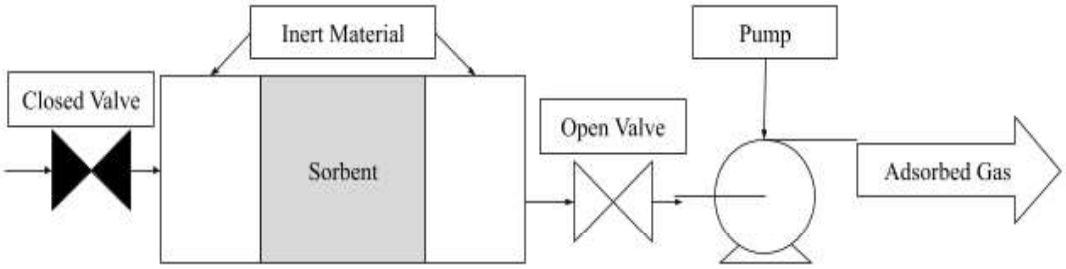

Figure 6: General Apparatus of Pressure Swing Adsorption

For studies on direct air capture of CO_2, there would also be a CO_2/relative humidity probe attached to the outlet of the bed to measure the concentrations of CO_2 and water at set time intervals to determine the desorption. Once the bed has been degassed, a breakthrough experiment can be initiated. This is done by using flow regulators on the various gas components to achieve the desired inlet concentration for each. Similarly, to the degassing procedure, there is also a CO_2/humidity probe attached to the outlet stream to measure the concentration of CO_2 and water as a function of time to measure the

breakthrough performance. A typical PFD of a breakthrough experiment can be seen below in Figure 7.

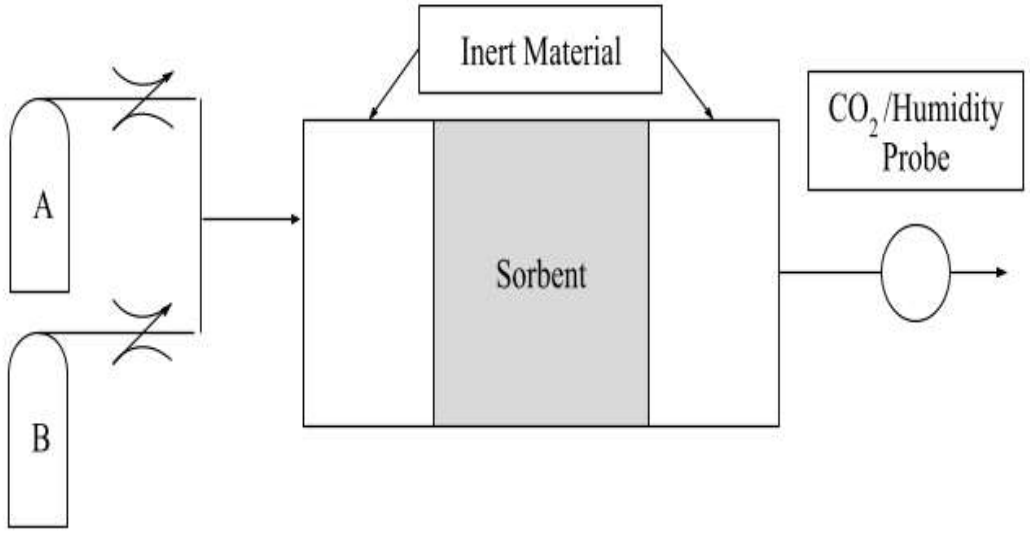

Figure 7: General Apparatus of a Breakthrough Experiment

How well a sorbent can adsorb a particular chemical species is dependent on several factors. The most impactful factors on a breakthrough point are the sorbent maximum adsorption capacity for a particular component, the inlet concentration of the component(s), the pressure of the PBR, the length of the PBR, the void fraction of the PBR, the density of the sorbent, and the mass transfer coefficient[25]. The maximum adsorption capacity is dependent on the sorbents' physical and chemical properties and can be measured using an adsorption isotherm that will be discussed further in future chapters. The inlet concentration of the component(s) is crucial because it will impact the mixed gas adsorption which is typically measured with ideal adsorbed solution theory (IAST) models[26]. The pressure of the PBR will dictate the maximum quantity adsorbed by the sorbent and is again measured using an adsorption isotherm. The length of the

PBR will affect the diffusion through the bed with longer beds having a longer breakthrough time and smaller beds having a shorter breakthrough time. The void fraction of the bed determines how much of the PBR is occupied by a sorbent. Meaning the larger the void fraction, the less volume is occupied by a sorbent which will decrease the breakthrough time. Density is conjoined with a void fraction: the denser the sorbent the more mass per volume the sorbent will have. However, both physisorption and chemisorption occur on the surface of the sorbent so maximizing surface area will increase the breakthrough time[27]. Much like the maximum quantity adsorbed, the mass transfer coefficient is dependent on the physical and chemical properties of the sorbent. This can be modeled and measured using Fick's law of adsorption which will be discussed further in future chapters. A general model of ideal breakthrough adsorption behavior can be seen in Figure 8 below.

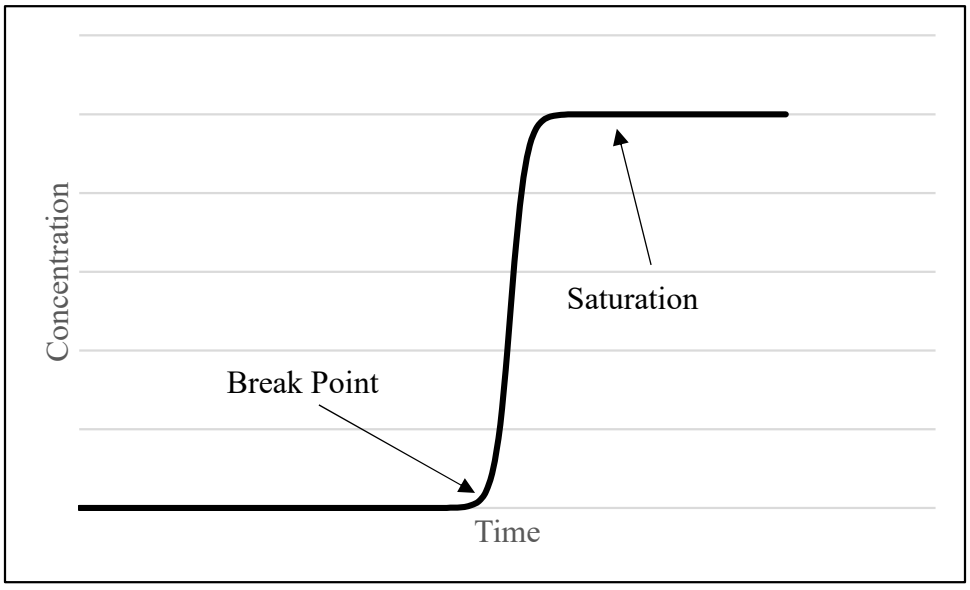

Figure 8: Ideal Breakthrough Adsorption Behavior

2.2 Governing Equations of Breakthrough

2.2.1 Adsorption Isotherm

Adsorption isothermal is a process of exposing set increments of a particular component to a sorbent at constant temperature and measuring the amount the sorbent was able to adsorb of the component. Using this data at discrete pressure or concentration points, a model can be derived that can predict the quantity adsorbed at any given pressure between the ranges of the pressures or concentrations that were measured. One of the most used equations for determining the adsorption isotherm is the Langmuir model as depicted below[28].

$$q_i^* = q_{m,i}\frac{b_i p_i}{1 + b_i p_i} \tag{2.1}$$

Where q^*_i is the equilibrium concentration, q_i is the quantity adsorbed, q_m is the max quantity adsorbed, b_i is the empirically derived constant, and p_i is the pressure of the system. The equation is empirically derived by using isotherm adsorption data and changing the value of b to minimize the least squared difference between the pressure values. More rigorous models that can fit data at a wider pressure range are the Freundlich isothermal model and the Langmuir-Freundlich or Sips model shown respectively below[29,30].

$$q_i = b_i {p_i}^{\frac{1}{n_i}} \tag{2.2}$$

$$q_i^* = q_{m,i}\frac{b_i {p_i}^{1/n_i}}{1 + b_i {p_i}^{1/n_i}} \tag{2.3}$$

Where n is another empirically derived constant used to fit the data. The Langmuir-Freundlich isotherm model is a combination of the Langmuir and Freundlich isotherm models.

2.2.2 Adsorption Kinetics

Adsorption kinetics is the measurement of diffusion in a system with respect to time[31].

$$\frac{\partial q}{\partial t} = \frac{1}{r^2}\frac{\partial}{\partial r}\left(r^2 D_c \frac{\partial q}{\partial r}\right) \tag{2.4}$$

Where q is the quantity adsorbed, r is the radius, D_c intracrystalline diffusivity. A simplification can be made to this model based on Fick's second law of diffusion which eliminates the directional component known as the linear driving force (LDF) model[32-34].

$$\frac{\partial \mathrm{q_i}}{\partial \mathrm{t}} = \mathrm{K_{p,i}}(\mathrm{q_i^*} - \mathrm{q_i}) \tag{2.5}$$

Where $K_{p,i}$ is the mass transfer coefficient comprised of the intracrystalline diffusivity and the adsorbent particle radius. More commonly, $K_{p,i}$ is empirically derived using experimental kinetic data.

2.2.3 Mass Balance

The mass balance is the means of calculating how the concentration of the component(s) being adsorbed by the sorbents. The concentration is dependent on both time and distance along the bed. The overall mass balance can be seen below[35].

$$u\frac{\partial c_i}{\partial z} + \frac{\partial c_i}{\partial t} + \frac{1-\epsilon}{\epsilon}\rho_p \frac{15 D_e}{R_p^2}\left(\frac{\partial q_i}{\partial t}\right) = 0 \tag{2.6}$$

Where ε is the total void fraction, c_i is the concentration of component i, u is the superficial velocity, ρ is the density of the bed, D_e is the intracrystalline diffusivity, and R^2_p is the adsorbent particle radius.

2.2.4 Energy Balance

The energy balance is the means of calculating the energy density per unit volume of the bed. It is dependent on the time and the position along the bed. The overall energy balance of a PBR can be seen below.

$$\frac{\partial \tilde{u}}{\partial t} = \varepsilon_b \frac{\partial}{\partial z}\left(\rho D \frac{\partial h}{\partial z}\right) - \frac{\partial v \rho h}{\partial z} + \frac{1}{1000}\frac{\partial}{\partial z}\left(\lambda_{eff}\frac{\partial T}{\partial z}\right) - \frac{4}{d_b}\frac{1}{1000}k_{T,b-w}(T - T_w) \quad (2.7)$$

Where ũ is the energy density per unit volume of the bed, ε is the bed void fraction, D is the axial mass dispersion coefficient, ρ is the density of the gas component, h is the specific enthalpy of the gas component, λ_{eff} is the effective thermal conductivity, d_b is the diameter of the bed, $k_{T,b-w}$ is the heat transfer coefficient between the wall and the gas component, T is the gas temperature, and T_w is the wall temperature. With respect to the specific enthalpy of the gas component, it can be calculated as a function of the temperature of the gas component shown below.

$$h_{ad,i}(T) = h_i^{\emptyset}(T) + \Delta H_{ad,i} + \Delta C_{p,ad,i}\left(T - T_{ref}\right) \quad (2.8)$$

Where $h_i^{\emptyset}(T)$ is the enthalpy at the temperature of the bed, $H_{ad,i}$ is the heat of adsorption for the gas component, and $C_{p,ad,i}$ is the difference in heat capacity of the adsorbed species. Additionally, in regard to the overall energy balance equation, the value of the effective thermal conductivity can be calculated with the following equation.

$$\lambda_{eff} = \varepsilon_b \lambda + (1 - \varepsilon_b)\frac{1}{\frac{0.22{\varepsilon_b}^2}{\lambda} + \frac{2}{3}\lambda_{ads}} \quad (2.9)$$

Where λ is the gas mixture's thermal conductivity, and λ_{ads} is the adsorbent material's thermal conductivity.

2.2.5 Momentum Balance

The momentum balance is means of calculating the pressure drop across the bed. In this case, it can be modeled as the Ergun equation as shown below[36].

$$\frac{\partial p}{\partial z} = -\frac{150\mu}{d_p^2}\frac{(1-\varepsilon_b)^2 v}{{\varepsilon_b}^3} - \frac{1.75\rho}{d_p}\frac{(1-\varepsilon_b)}{{\varepsilon_b}^3}u^2 \tag{2.10}$$

Where μ is the dynamic viscosity of the gas component and d_p is the diameter of the sorbent.

2.3 Assumptions and Final Equations

For the simulation model, the overall assumption was that it was a linear driving force approximation (LDF). The other assumptions that went into this model were that the system is isothermal across the entire bed, so an energy balance was not required. There is negligible pressure drop across the bed, so the Ergun equation was not needed. The Langmuir isotherm is constant for the entire bed. The system operates as an ideal plug flow reactor (PBR) where the flow is entirely linear with no radial or axial dispersion. There are no fouling factors or other contaminants in the bed. These assumptions are all valid for n number of components at the inlet.

The adsorption kinetics based on Fick's Law is similar to equation number 2.5. The isotherm is based on the extended Langmuir isotherm as follows[37].

$$q_1^* = \frac{q_{m1} b_1 P_0 (1 + b_2 * P_0)}{1 + y_1[L,t] P_0 (b_1 - b_2 + b_1 P_0)} \tag{2.11}$$

$$q_2^* = \frac{q_{m2} b_2 P_0 (1 + b_1 * P_0)}{1 + y_1[L,t] P_0 (b_1 - b_2 + b_1 P_0)} \tag{2.12}$$

Where q_i^* is the quantity of each component in kilograms adsorbed per kilogram of absorbent, q_{mi} is the maximum quantity adsorbed of each component in kilograms per kilogram of absorbent, b_i is the Langmuir constant of each component, y_1 is the concentration at a given time in kilograms per cubic meter, and P_0 is the pressure of the bed in kPa.

The mass transfer kinetics based on Fick's law at a given point in time and length is determined by the following questions.

$$\frac{\partial q_1}{\partial y} = 1 + \frac{1-\epsilon}{\epsilon} * \frac{\rho RT}{P_0} * ((1 - y_1[L,t]) * q_1^* + y_1[L,t] * q_2^*) \tag{2.13}$$

$$\frac{\partial q_2}{\partial y} = -\left(\frac{1-\epsilon}{\epsilon}\right)^2 * \frac{\rho RT}{P_0} * (q_1^* + q_2^*) \tag{2.14}$$

Where $\frac{\partial q_i}{\partial y}$ is the adsorbed phase concentration at a given time and bed length, R is the universal gas constant in units of $(\frac{kPa* L}{mol*K})$, T is the temperature in units of K, and ρ is the framework density in units of kg/L.

The mass balance of the system can is represented by the following PDEs.

$$\mathrm{u}^* = \mathrm{u}[\mathrm{L}, \mathrm{t}-1] + \Delta L * \frac{\partial q_2}{\partial y} * u[L, t-1] * \frac{\epsilon}{\left(\frac{\partial q_1}{\partial y}\right)} * \frac{y_1[L,t] - y_1[L,t-1]}{\Delta L} \tag{2.15}$$

$$\mathrm{C}_1 = y_1[L,t] - \frac{\Delta t * u^* * \epsilon}{\left(\frac{\partial q_1}{\partial y}\right)} * \frac{y_1[L,t] - y_1[L,t-1]}{\Delta L} \tag{2.16}$$

Where u^* and u are the corrected superficial velocity and superficial velocity respectively both with units of m/s, ΔL is the discretizational step size of the bed length, ϵ is the bed void fraction, and $\left(\frac{\partial q_1}{\partial y}\right)$ is the change in concentration.

The boundary and initial conditions were chosen so that it assumes that the system is completely purged prior to the initial startup. The boundary conditions of the simulation are as follows.

$$c_i = c_{i0} \qquad z = 0,\ t = 0$$

This boundary condition is specifying that the inlet concentration is equal to the concentration of the system at zero distance and zero time to initialize the system. This will be visualized further in the numerical methods section. The initial conditions of the simulation are as follows.

$$c_i = c_{i0} \qquad z = 0,\ t = 0$$

$$q_i = 0 \qquad 0 < z \leq L,\ t = 0$$

$$c_i = 0 \qquad 0 < z \leq L,\ t = 0$$

The initial conditions are specifying that the concentration of the system is equal to the inlet concentration at the inlet at time zero and is zero at all other lengths at time zero. Additionally, it is specifying that the quantity adsorbed is zero at time zero at all lengths.

2.4 Numerical Methods

The finite element method is a means of solving a numerical solution of a partial differential equation[38]. It is employed by creating a grid of discretized nodes. Each node is then evaluated by replacing the derivative with finite-divided differences. Essentially the process creates a point-wise function to approximate the values of the analytical solutions. This is comparable to Euler's method for solving for numerical solutions of a derivative however, Euler's method is limited to solving for only a one-dimensional case whereas the finite element method can work in N-dimensions. Because this method produces a numerical solution instead of an analytical solution, to obtain accurate results

the discretization step sizes must be as small as possible. If step sizes are too large, then the solution diverges from the analytical solution. This can be visualized in figures 9 and 10 below.

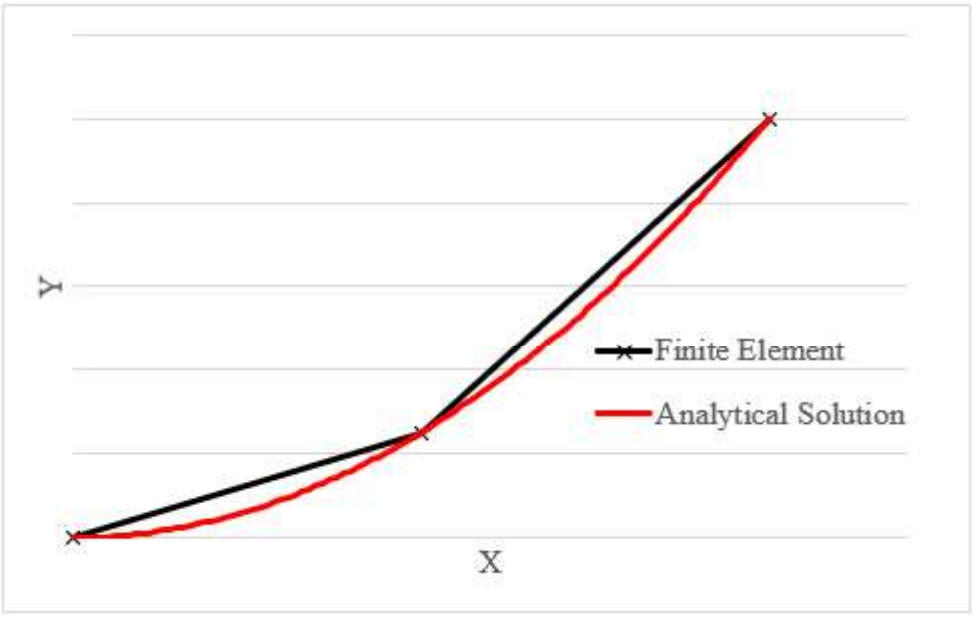

Figure 9: Poor Step Size for Finite Element Method

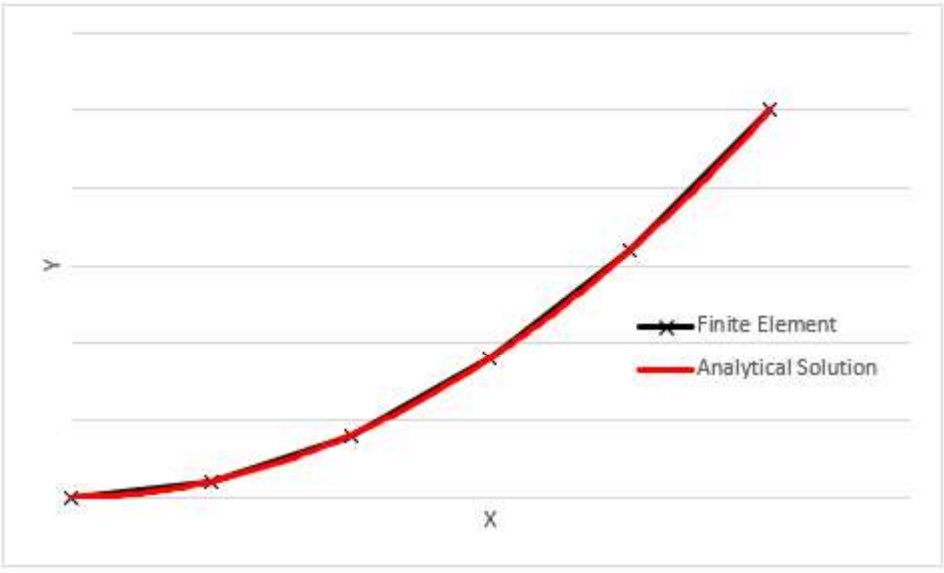

Figure 10: Good Step Size for Finite Element Method

Along with discretization, this method also requires initial and boundary conditions to compute values. Initial conditions determine the overall values across the system. For example, for this study as previously discussed, the bed is initially assumed to be empty, and the inlet concentration is equal to the maximum concentration of the bed.

The overall problem was to solve for concentration at the outlet as a function of time. This was done by combing equations 2.15 and 2.16 into the following coupled partial differential equations (PDE).

The general approach for solving this coupled PDE was to utilize the finite-element method which uses forward and backward approximations of the integral to solve for the current value of concentration and quantity adsorbed. First, the values of time and distance needed to be discretized into small step sizes to create a mesh. Then empty arrays were generated with the initial and boundary conditions in mind for the number of components that resembles something like Figure 11 below.

Distance

Time

$$\begin{bmatrix} C_{i0} & 0 & \cdots & 0 \\ \vdots & 0 & \ddots & \vdots \\ C_{i0} & 0 & \cdots & 0 \end{bmatrix}$$

Figure 11: Initializing Matrix for the Concentration of Size M X N Where M Is the Change in Time, N Is the Change in Distance, and Matrix Values Are the Concentration of Component i

Similarly, to the initializing matrix for concentration, the quantity adsorbed matrix is also of size M x N, however, it is initialized as a zero matrix as shown in figure 12 below.

Distance

Time $\begin{bmatrix} 0 & \cdots & 0 \\ \vdots & \ddots & \vdots \\ 0 & \cdots & 0 \end{bmatrix}$

Figure 12: Initializing Matrix for Quantity Adsorbed of Size M X N Where M Is the Change in Time, N Is the Change in Distance, and Matrix Values Are Quantity Adsorbed of Component I

Once the matrices were set up, then the following equations were used to solve for the numerical solution.

For the other model, it utilized both least squared regression and the 'fsolve' optimization function. Least squared regression is numerical method that can determine the absolute deviation between two points fitting the form shown in equation 2.17 below.

$$Least\ Squares = (a - b)^2 \tag{2.17}$$

Where 'a' is the value of the first line and 'b' is the value of the second line. Using this methodology, a standard breakthrough curve will fit a B-A model as shown in equation 2.18 below[39].

$$\frac{C}{C_0} = \frac{1}{1 + e^{a-bt}} \tag{2.18}$$

Where C and C_0 are concentrations, a is constant dependent on the mass transfer coeffient, adsorption capacity of the bed, the bed length, and the superficial velocity, and 'b' is a constant dependent on the mass transfer coefficient and the inlet concentration. The the least squares regression compares values from experimental data and those modeled by equation 2.18 which will be explored more in future chapters.

CHAPTER 3

MODELS FOR EXPERIMENTAL ADSORPTION BREAKTHROUGH DATA AND PREDICTED ADSORPTION BREAKTHROUGH BEHAVIOR

3.1 Model I: Fitting Experimental Data to Ideal Breakthrough Behavior

3.1.1: Inputs

Once the program has been started, the program asks for three different inputs for the program to run. The first is the experimental data from a .csv file which fits the following template shown in Table 3 below.

Table 3: Template of imported .csv file of experimental data

Time	PPM
t_1	PPM_1
…	…
t_{final}	PPM_{final}

The template format must be followed exactly, the program will not recognize the column data types without the properly formatted headings with the proper capitalization. The next piece of information the program will ask for is the inlet concentration of the measured component. The final piece of information it will ask is an initializing guess of the ‘a’ and ‘b’ parameters. Typically, a guess of ‘1’ for both ‘a’ and ‘b’ is sufficient. The program then splits the data provided from the experimental data file into time and concentration arrays. Then all the indices in the concentration array are divided by the inputted inlet concentration.

3.1.2: Sigmoid Function

As previously mentioned in chapter 2, the function that this code uses to fit the empirical data is a standard B-A model which resembles an S-shaped sigmoid function as shown in equation 2.16. The program passes three variables into this function which are time, the 'a' constant, and the 'b' constant.

3.1.3: Curve Fitting

The curve fitting function is built into the scipy.optimize python package calls for five pieces of information to run[40]. A function, experimental x values, experimental y values, initial guesses, and bounds of possible values. The function is the shape that the curve will attempt to fit, in this case, it is the sigmoid function. The experimental x and y values came from the imported experimental data file. The initial guesses came from the inputted guesses by the user. The bounds are permanently set to values of $0 < a, b < \infty$. The curve fit function works by creating a least squared regression between the experimental data and the calculated data points. Then it uses a 'fsolve' function which changes the values of 'a' and 'b' to get an optimized solution at a single point. In this case, it is trying to optimize the summation of the least squared difference to a value of 0. Since experimental data is not going to produce a perfect B-A model and fit the sigmoid shape perfectly, the program will attempt to output values of 'a' and 'b' that produce the smallest summation value of the least squared difference.

3.1.4 Outputs

The outputs of the model are the values of 'a' and 'b' and a graph. The graph has two different data sets on it. The first data set is a scatter plot of the experimental data, and the

second data set is a solid line of the function with the computed ‘a’ and ‘b’ values. An overview of how the entire code can be seen below in Figure 13.

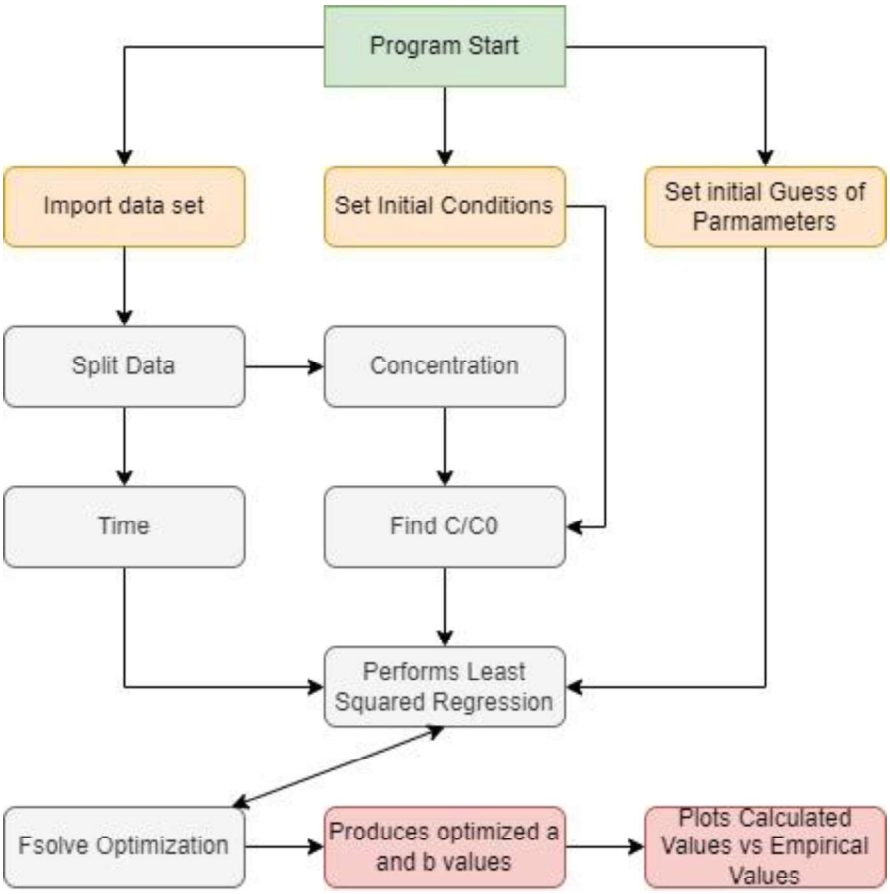

Figure 13: Flowchart of Model I Where Orange Blocks Are Inputs by the User, Grey Blocks Are the Code Being Executed, and Red Blocks Are the Program Outputs

3.2: Model II Predicted Adsorption Breakthrough Behavior

3.2.1: Inputs

Once the program is initiated, it will require four sets of data: experimental data, material properties, bed parameters, operating conditions, and runtime. The first set of data is experimental data. This input has no impact on the model itself, it is only for validation purposes. The material properties include information regarding the IAST data for the gas

components and the framework density of the adsorbent. The IAST data asks for the saturation loading concentration of each gas component and the Langmuir 'b' constant. The bed parameters and operating conditions ask for the temperature, the starting pressure, bed diameter, bed length, bed void fraction, and inlet flow rate of the gas components. The final input asks for the maximum breakthrough dimensionless time. This will need to be manually changed by the user since the program is not currently set up to stop automatically stop once the bed reaches saturation.

3.2.2 Discretization, Initial Conditions, and Boundary Conditions

As previously discussed in chapter 2, the model is set up to solve partial differential equations (PDE) by using the finite difference method which essentially solves for the change of one element with respect to multiple elements. In this case, the PDEs are set up to solve for the change in concentration with respect to time and change in bed length. The matrices are set up in size [Dimensionless Bed Length x Dimensionless Time]. Dimensionless bed length is normalized on a scale from zero to one with zero being the inlet and one being the outlet of the bed. The dimensionless time is preset by the user in the inputs. Table 4 below shows the components and their size.

Table 4: Initialized Matrix Components and their size

Matrix Name	Size
Time	[Dimensionless Time x 1]
Pressure of Component i	[Dimensionless Time x Dimensionless Bed Length]
Mole Fraction of Component i	[Dimensionless Time x Dimensionless Bed Length]
Superficial Velocity	[Dimensionless Time x Dimensionless Bed Length]

Initial conditions are amendable by the user but are default set to the bed being void of all gas components. The boundary conditions are set so that at time zero and bed length zero the bed is saturated with the gas components.

3.2.3: PDE Solver

The PDE solver is set up as a for-loop to calculate the value of concentration as a function of both time and bed length. The first step solves for the maximum quantity adsorbed by each gas component using a Langmuir isotherm for multiple components as shown in equations 11 and 12. Next, the actual quantity adsorbed of each component is calculated using equations 13 and 14. The next step solves for the change in superficial velocity across the bed using equation 15. The last step then solves the concentration of a gas component at the outlet as a function of time using equation 16. The for-loop will then restart at the next dimensionless time value and continue until the maximum breakthrough time has been reached. Once the for-loop terminates it will plot the change in concentration at the outlet as a function of time vs the experimental data provided by the user in the input steps. Figure 14 below shows the overall process of the second model.

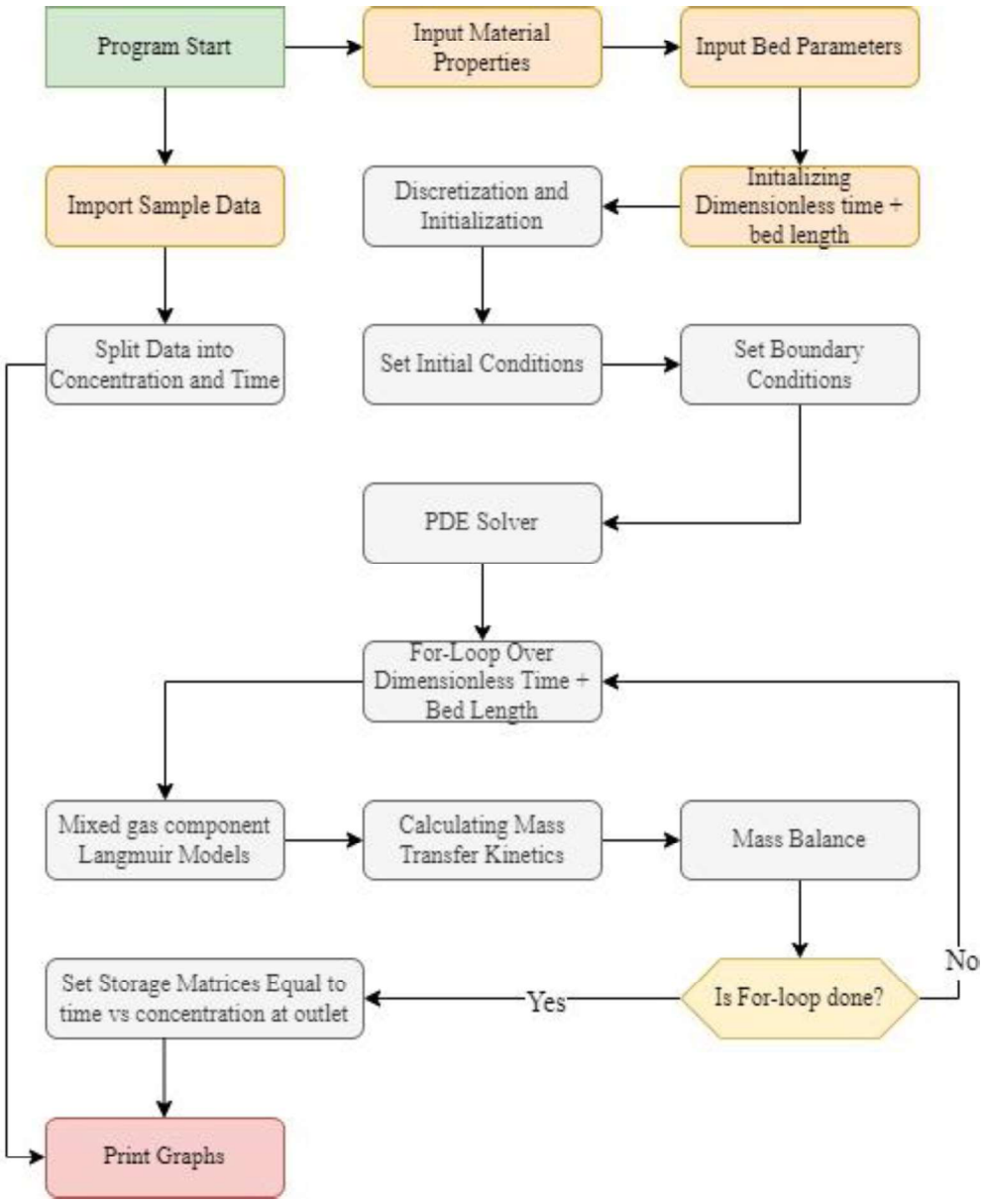

Figure 14: Flowchart of Model Ii Where Orange Blocks Are Inputs by the User, Grey Blocks Are the Code Being Executed, Red Blocks Are the Program Outputs, and Hexagons Are Decision Points for the Code.

CHAPTER 4

RESULTS AND DISCUSSION

4.1 Model I

4.1.1: Results of Fitting Data Program Case 1

The first test case that was analyzed was with experimental breakthrough adsorption data of AD-1 zeolite. The experimental data was given by Dr. Mai Xu and not tested by the author. The experimental conditions for this trial were conducted at standard temperature and pressure of 298K and 1 bar. The mixed gas composition was 415 parts per million (ppm) by volume of CO_2 and 2 liters per minute of N_2. The adsorbent mass in the packed bed was 4.1 grams.[41]

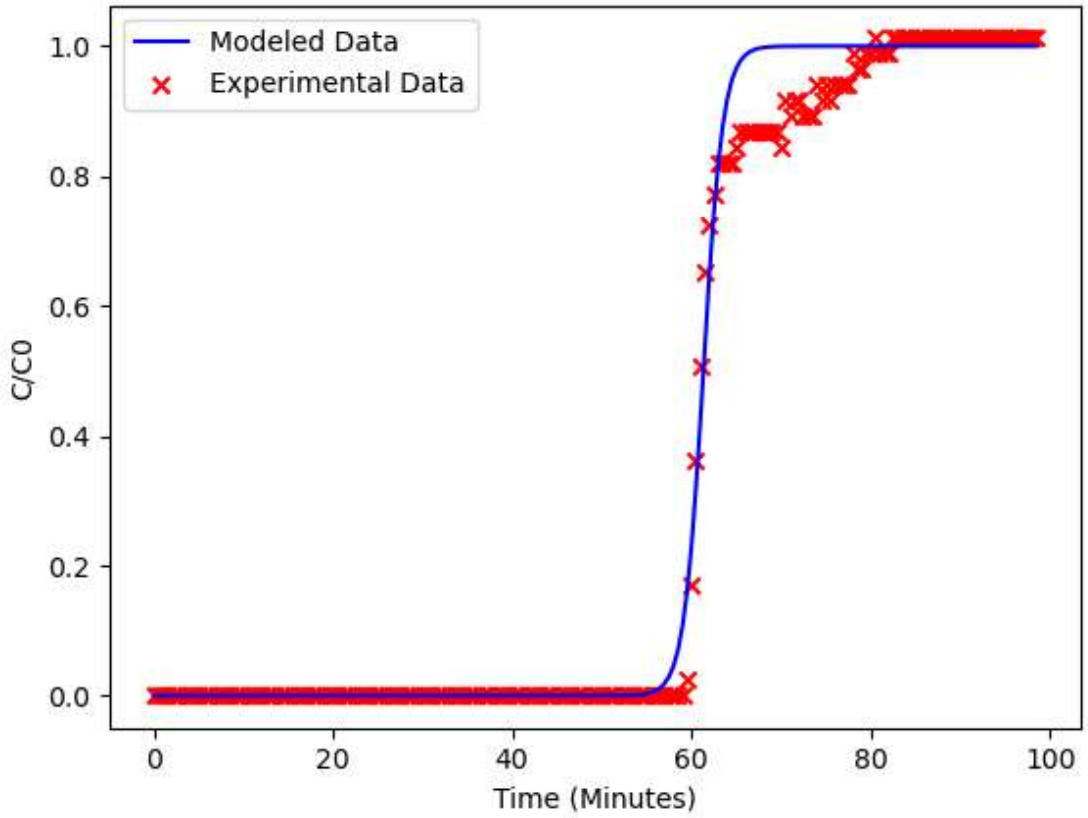

Figure 15: Breakthrough Fitting Model for Case 1

It can be seen in Figure 15 that the results of the code were successful for this case. The modeled data was able to effectively mimic the breakthrough behavior. A t-test was used to validate the model's accuracy and the t-value was 4.2526×10^{-6} which is below the standard 0.05 value which validates this model's accuracy. The areas with the greatest discrepancies between the experimental data and the model were at the end of the initial upshoot in CO_2 concentration and at the absolute saturation point at the end which read 420 PPM for the experimental data. This model can be compared to the gPROMs model for the same experiment provided by Dr. Mai Xu[41].

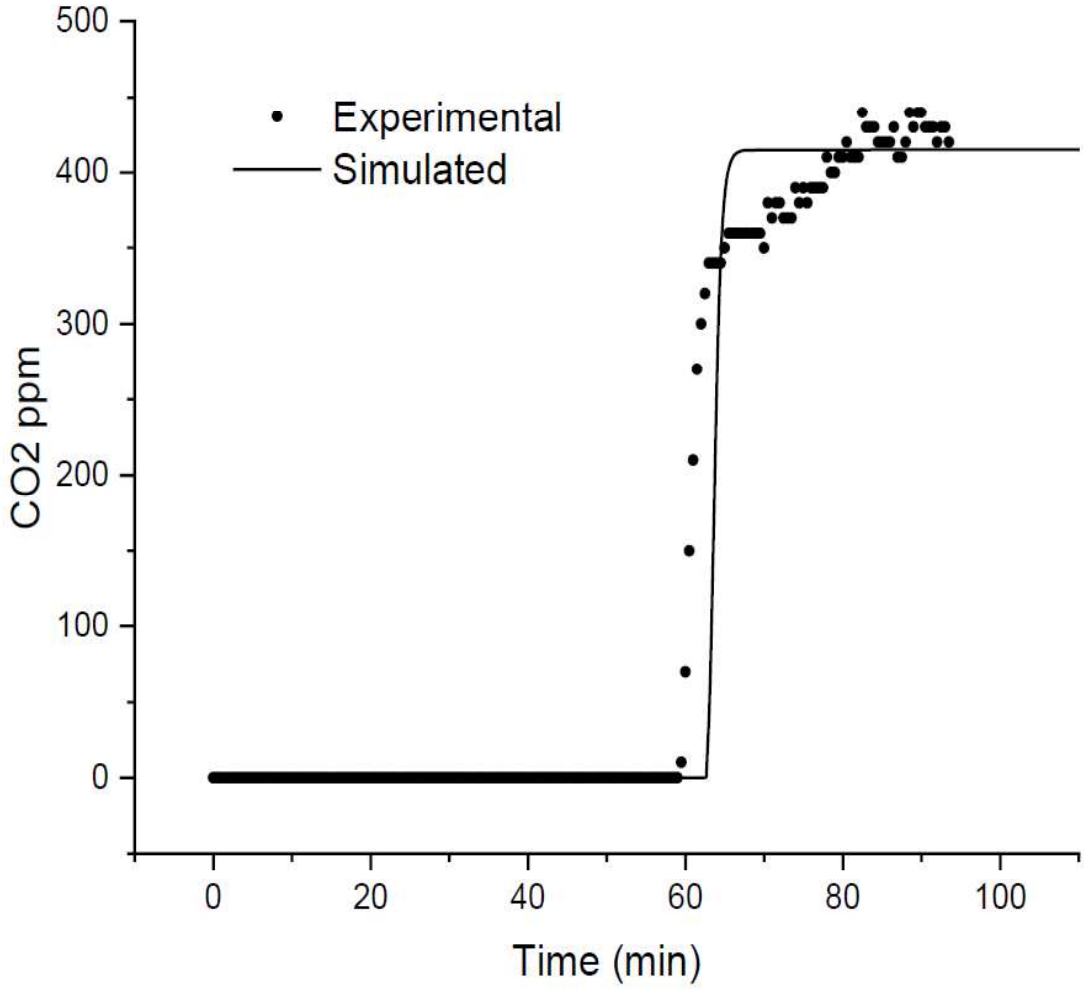

Figure 16: Breakthrough Model for Case 1 Using gPROMs[41]

When comparing Figure 15 with Figure 16, it can be seen that the fitting model slightly underestimated the breakpoint to be ~55 minutes and the gPROMs model slightly overestimated the breakpoint to be ~62 minutes. The experimental breakpoint appears to be ~60 minutes. The gPROMs model also appears to resemble more of a step function rather than a more typical sigmoid shape that has a less steep slope. This makes the gPROMs model less realizable for this case.

4.1.2: Results of Fitting Data Program Case 2

The next case that will be examined comes from the author's undergraduate thesis[42]. A nanostructure NaX zeolite was used as the adsorbent. The experimental conditions for this trial were conducted at standard temperature and pressure of 298K and 1 bar. The mixed gas composition was 500 parts per million (ppm) by volume of CO_2 and 2 liters per minute of N_2. The adsorbent mass in the packed bed was 7.183 grams.

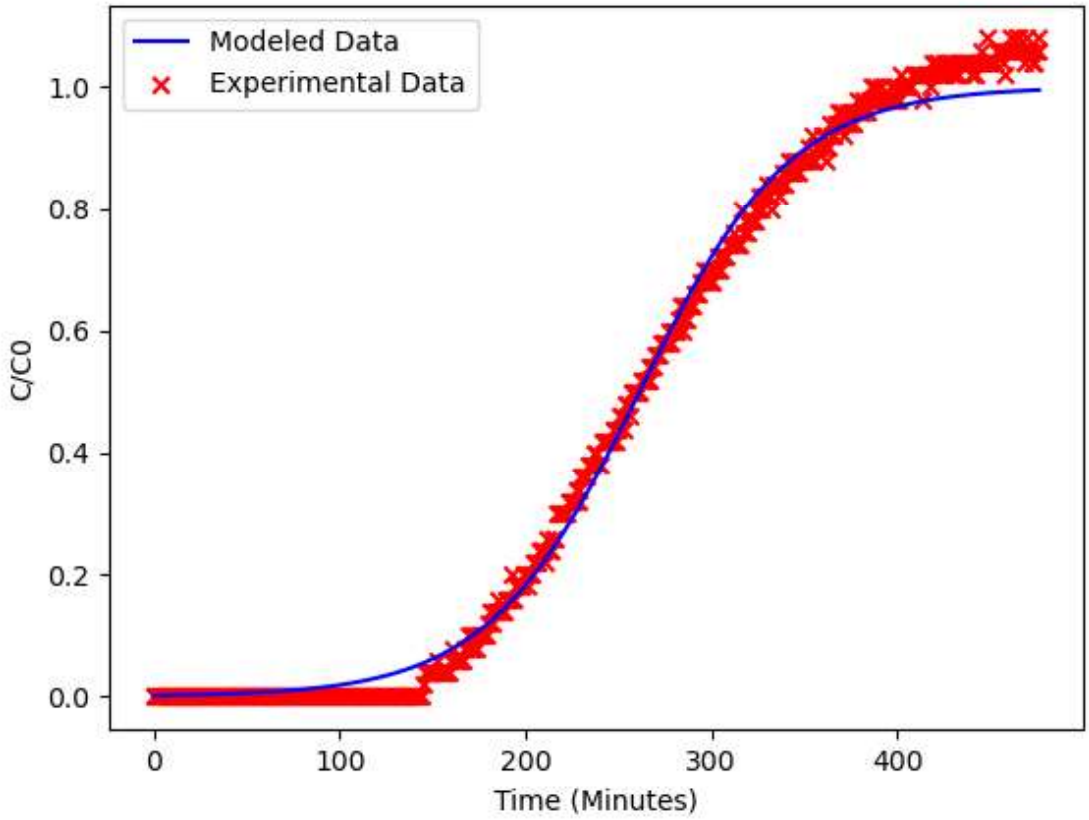

Figure 17: Breakthrough Fitting Model for Case 2

It can be seen in Figure 17 that the breakthrough experiment did not exhibit ideal breakthrough behavior with the concentration of the outlet steadily increasing for ~250 minutes. Likewise, the model mimicked the same trend produced by the experimental data. Additionally, in this case, it had similar problems as case 1 in underestimating the breakpoint early. This model was highly accurate to the test data producing a t-value of 0.024784 which is below the standard 0.05 value for statistical significance.

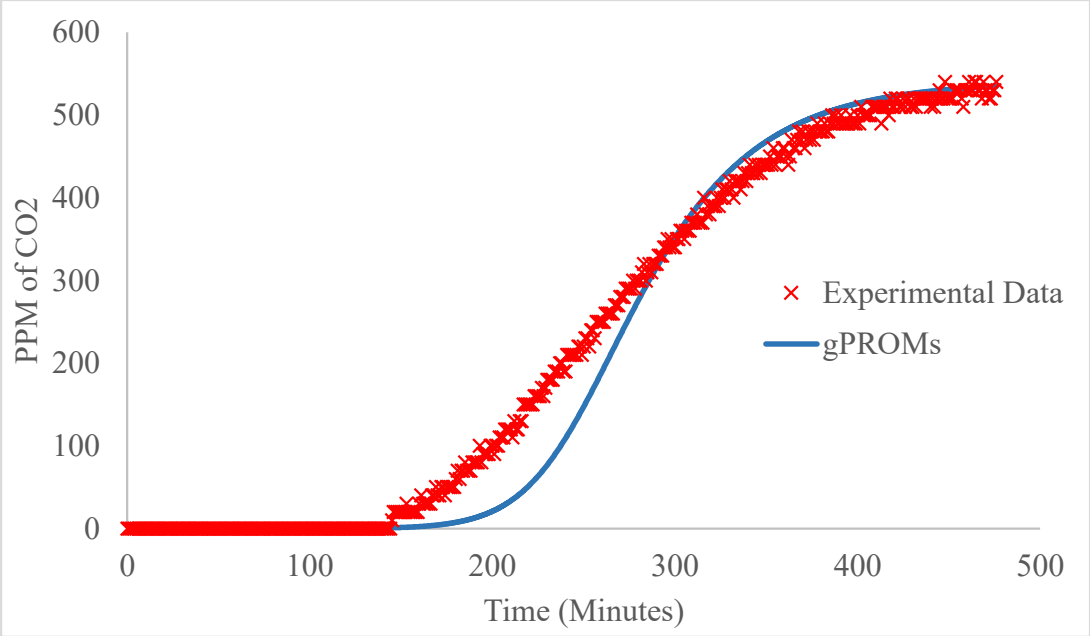

Figure 18: gPROMs Breakthrough Model for Case 2 [42]

The gPROMs model from Figure 18 for this case had similar problems as the fitting model. Due to the unideal behavior of the experimental data the gPROMs were not able to produce a more standard breakthrough curve. Comparing the two models for this test data yielded similar results as the first test case. The fitting model underestimated the breakpoint and the gPROMs overestimated the breakpoint by ~50 minutes and ~25 minutes respectively. The gPROMs model did a significantly better job for this case in regard to predicting the breakpoint.

Overall, the fitting model performed well. It was able to accurately mimic experimental data shape and if the breakthrough behavior is closer to ideal it did a good job of predicting the breakpoint. The flaws in the model can be summarized in two points. Firstly, the model seems to favor an earlier breakpoint to adhere more closely to the sigmoid shape. Secondly, the model is dependent on experimental data having ideal

breakthrough behavior. The less ideal the experimental data, the more incorrectly the fitting model will predict the breakpoint.

4.2 Model II

4.2.1: Results of Predicting Data Program Case 1

The first test case for this program utilizes data from Dr. Joshua Thompson's dissertation[37]. His data was only reported in dimensionless time, so the predicting model was adjusted to be kept in dimensionless time and report mole fraction at the outlet instead of concentration divided by inlet concentration. The input parameters can be seen in Table 5 below.

Table 5: Case 1 Model Parameters

Parameter	Value
Saturation Loading of Component 1	12.2 mol/kg
Saturation Loading of Component 2	12.2 mol/kg
Langmuir Constant of Component 1	0.000618 1/kPa
Langmuir Constant of Component 2	0.000223 1/kPa
Framework Density	0.983 kg/L
Temperature	298.15 K
Pressure	1000 kPa
Component 1 Molar Fraction	0.5
Component 2 Molar Fraction	0.5
Bed Void Fraction	0.4
Superficial Velocity	1 m/s
Maximum Breakthrough Time	35

The simulation was testing a 50:50 molar fraction split between CO_2 and CH_4. The comparison in results from the predictive model and the Thompson model can be seen below.

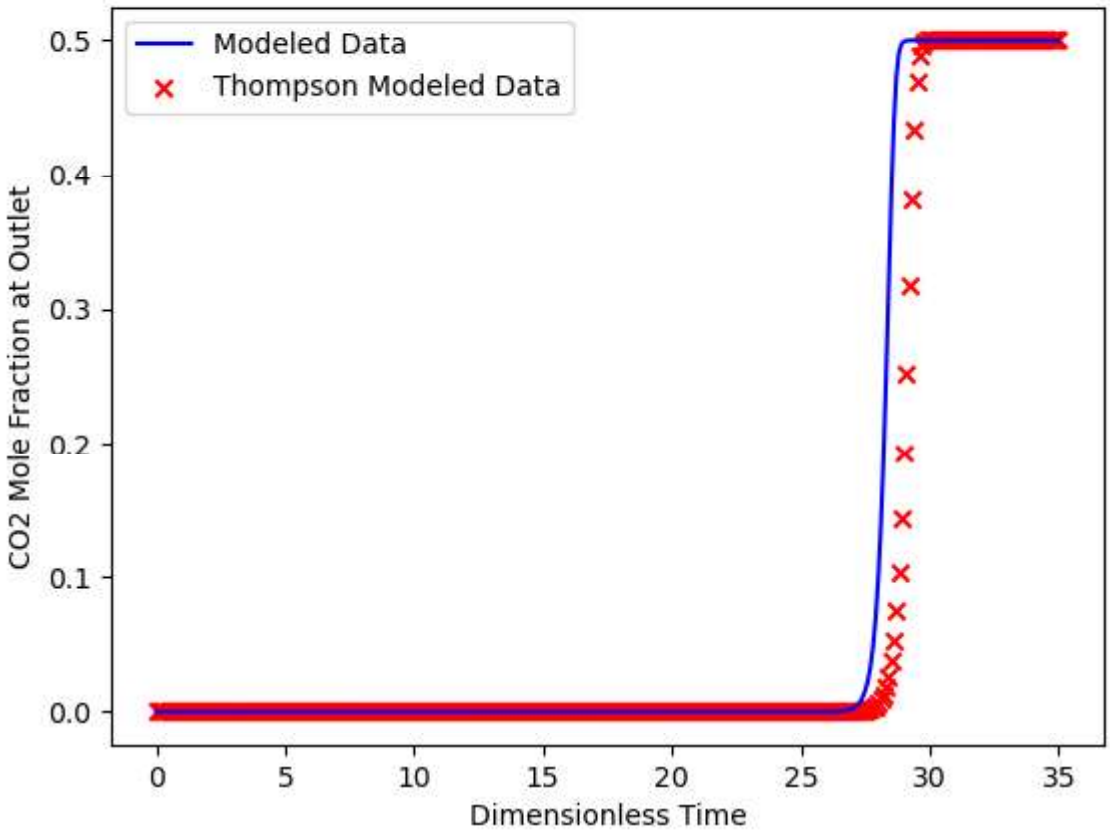

Figure 19: Breakthrough Behavior Prediction Case 1

The results in Figure 19 of the two models were extremely similar. The only difference between the two models is slight in the initial breakpoint. However, they maintained a very similar slope during the upshoot in concentration at the outlet and both reported the same saturation mole fraction of CO_2. These two models compute breakthrough behavior very similarly with the only difference being in the calculation in the first step in the PDE

solver which was calculating the maximum quantity adsorbed by the adsorbent. This model was highly accurate to the test data producing a t-value of 1.37166×10^{-18} which is well below the standard 0.05 value for statistical significance.

4.2.2: Results of Predicting Data Program Case 2

The next test case uses the same experimental data from the first test case of the fitting model. The saturation loading and the Langmuir constants were generated using pure component isothermal data using Trevor Ciha's IAST generation code[43]. That experiment and this model were carried out with the following parameters as shown in Table 6.

Table 6: Case 2 Model Parameters[41]

Parameter	Value
Saturation Loading of Component 1	101.5887 mol/kg
Saturation Loading of Component 2	63.6585 mol/kg
Langmuir Constant of Component 1	0.2985 1/kPa
Langmuir Constant of Component 2	0.001428 1/kPa
Framework Density	0.241 kg/L
Temperature	298.15 K
Pressure	100 kPa
Component 1 Molar Fraction	0.0004
Component 2 Molar Fraction	0.9996
Bed Void Fraction	0.21
Bed Diameter	0.0127 m
Maximum Breakthrough Time	35
Flow Rate	0.0033 m^3/s
Bed Length	0.56

The simulation was for a 200 mL/min flow rate of N_2 with a CO_2 concentration of 415 PPM. The results of the predictive model and the experimental results can be seen below.

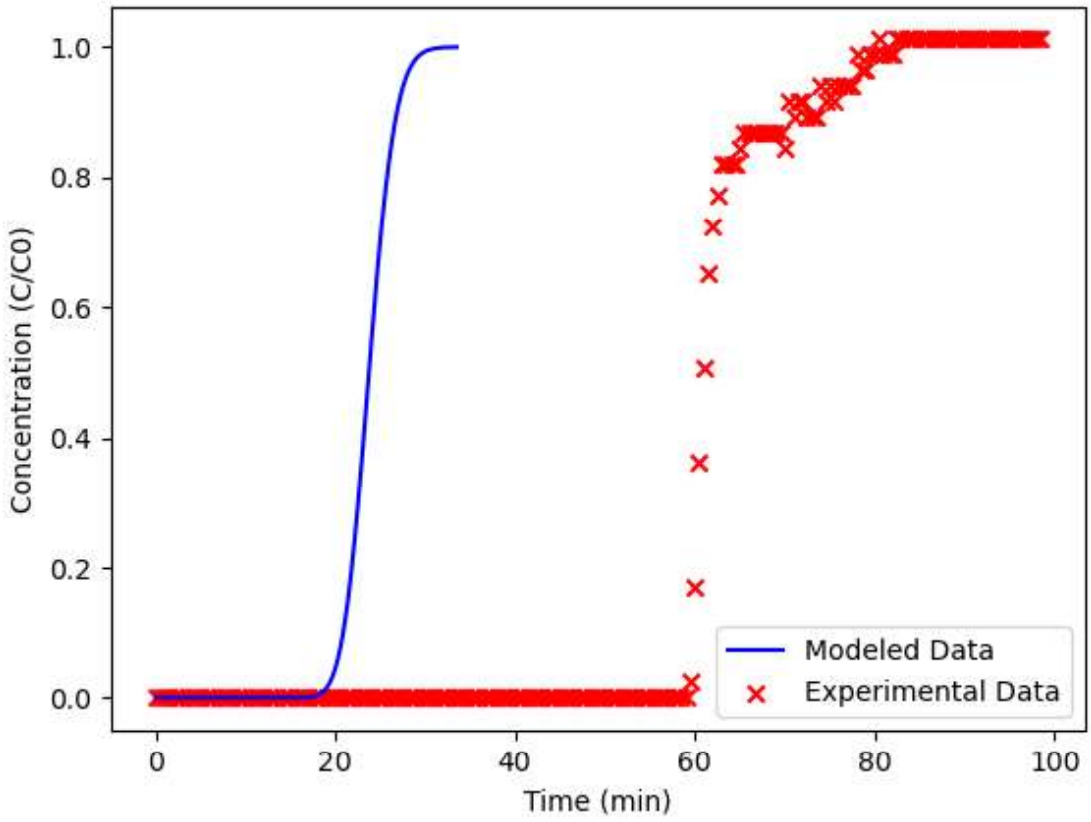

Figure 20: Breakthrough Behavior Prediction Case 2

The results shown in Figure 20 of this modeling attempt were unsuccessful. The breakpoint for this trial was significantly off by ~40 minutes. Due to the complex nature of the predictive model, it is difficult to determine exactly what caused the model to be so inaccurate. The main possibilities of error however are inaccurate pure isothermal data and incorrect measurements of the bed parameters. If the pure isothermal data was not accurate then it would change the saturation loading of each component and the Langmuir constants which would significantly impact the accuracy of the model due to their nature on the rest of the PDE solver. Those values appear in every step of the PDE solver. If the measurements of the bed parameters are incorrect, then it could significantly affect the calculation of the superficial velocity and conversion from dimensionless time

to real-time. Because the superficial velocity is calculated by the flow rate divided by the cross-sectional area of the PBR, the overall rate at that components are entering the bed could be significantly different. Additionally, the conversion from dimensionless time to real-time is also heavily impacted by the space velocity. Overall, it is uncertain as to what caused the model to reach the breakpoint so early.

To correct for this discrepancy in breakthrough time, the superficial velocity was reduced by a factor of 3 as shown in Figure 21 below.

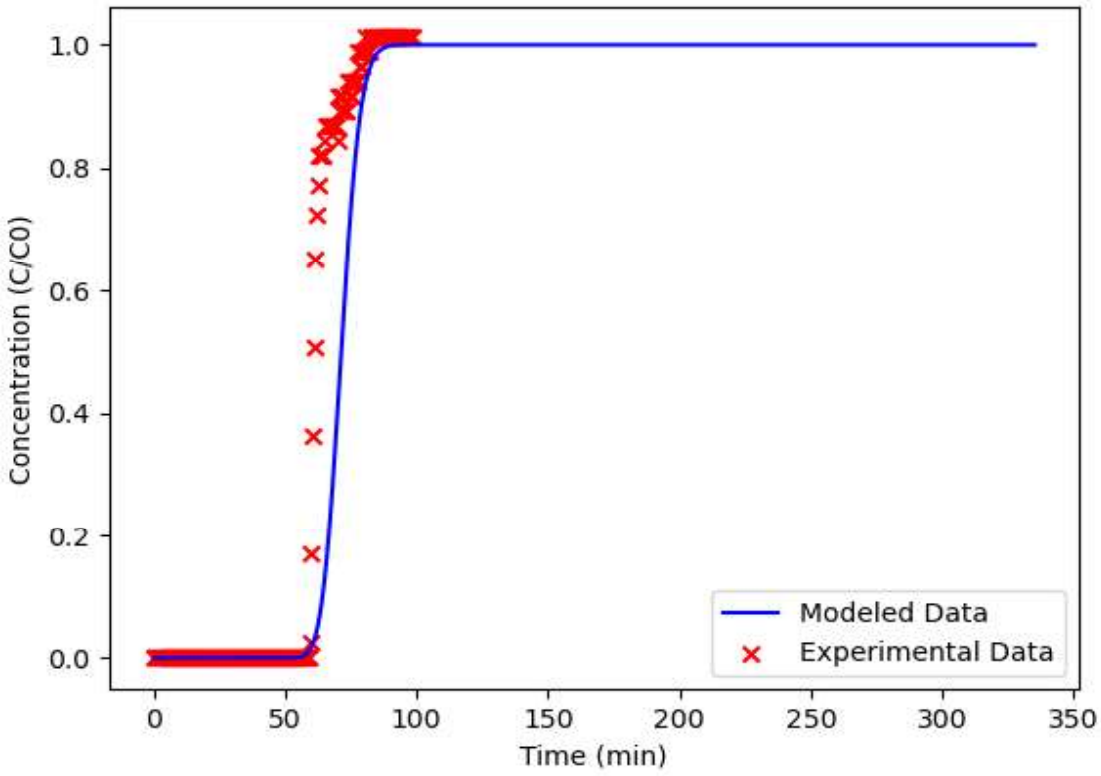

Figure 21: Model II Case 2 with a reduced superficial velocity of a factor of 3

Comparing the corrected superficial velocity from Figure 21 with the gPROMs model in Figure 16, the results are extremely similar. However, the gPROMs model still tends to overpredict the breakpoint and model II tends to underpredict the breakpoint. This model

was highly accurate to the test data producing a t-value of 1.44623×10^{-22} which is below the standard 0.05 value for statistical significance.

4.3: Model Comparison to gPROMs

Compared to gPROMs, the two models performed well. For model I, if the breakthrough behavior was ideal, it was able to accurately replicate the breakthrough curve with minimal underpredicting of the breakpoint and saturation time. The flaws of the Model I came from unideal breakthrough behavior shown in case 2. This caused the model to significantly underpredict the breakpoint. For model II, if the input parameters were accurate, it produced accurate results. The major flaw with model II is that it is dependent on a lot more variables than model I which can significantly alter results if all the inputs are not correct. Table 7 below summarizes the inputs, outputs, and results.

Table 7: Comparison between Model I, Model II, and gPROMs

	gPROMs	Model I	Model II
Inputs	• Experimental data • Isothermal Data • Bed length • Bed void fraction • Temperature • Pressure • Inlet concentrations • Flow rate • Bed cross-sectional area • Material density	• Isothermal Data • Bed length • Bed void fraction • Temperature • Pressure • Inlet concentrations • Flow rate • Bed cross-sectional area • Material density	• Experimental Data • Inlet concentration
Outputs	• Model of breakthrough behavior	• Model of breakthrough behavior	• Model of breakthrough behavior
Results	• Tends to overpredict breakpoint and saturation point	• Tends to underpredict breakpoint and saturation point	• Tends to underpredict breakpoint and saturation point

CHAPTER 5

SUMMARY AND FUTURE RECOMMENDATIONS

The two models were created for open-source usage in Python which is a free and easy-to-use program. The first model used experimental data to predict the ‘a’ and ‘b’ constants of a B-A model. Where a is composed of the mass rate constant, the adsorption capacity of the adsorbent, the superficial velocity, and the bed length, and b is composed of the mass rate constant and the inlet concentration of the adsorbed component. The second model used isothermal adsorption data, bed parameters, and operating conditions to predict the breakthrough behavior of a particular component.

The downsides of the first model were that if the sorbent did not exhibit typical breakthrough behavior, then the predictive model would only mimic that poor data and could not properly correct to a more ideal sigmoid shape. Additionally, the model currently can only calculate the ‘a’ and ‘b’ constants and is not set up to compute the individual variables of which they are composed. For future work, the hope is to have the model be able to extract the variable that ‘a’ and ‘b’ are composed of to improve the performance of the predictive model.

The downsides of the second model are that it currently requires priorly obtained mixed gas adsorption data. By working with other members of the Deng group who have created such a code, the two programs could run together to produce both IAST data and breakthrough behavior in a single program. Additionally, for the second model, the overall code could be improved in several ways. Firstly, the program currently takes an extended period to run even with fewer step sizes being analyzed. (Approximately 30 seconds for 100 steps). The current method is guessing the

dimensionless time, and bed length iterations required to reach total bed saturation. So, the model currently may undershoot or overshoot the number of iterations for the system to reach total saturation. The time could be reduced by having the program default to many iterations and having it automatically stop once the bed has reached total saturation. Additionally, the second model could be improved by combining it with the empirical model generated by the first model. This would be done replacing the theoretical trend for mass transfer kinetics used in the second model with empirically derivied mass transfer kinetics determined by the first model. Lastly, the second model's underlying assumptions of isothermal and isobaric conditions only apply because the PBR is assumed to be small enough to have neglibible energy and momentum changes. For future modifications to the model, it would include momonetum and energy balances so the model would apply to larger PBRs.

REFERENCES

[1]"Global Greenhouse Gas Emissions Data." EPA. Environmental Protection Agency, September 13, 2019. https://www.epa.gov/ghgemissions/global-greenhouse-gas-emissions-data.

[2]Natural Gas Combustion . https://www.epa.gov/sites/production/files/2020-09/documents/1.4_natural_gas_combustion.pdf.

[3]*Flue Gas—An overview | ScienceDirect Topics*. (n.d.). Retrieved April 5, 2022, from https://www.sciencedirect.com/topics/chemistry/flue-gas

[4]FLEDER RICHARDM. *ELEMENTARY PRINCIPLES OF CHEMICAL PROCESSES*. S.l.: JOHN WILEY; 2020.

[5]Climate Change Indicators: Atmospheric Concentrations of Greenhouse Gases. EPA. https://www.epa.gov/climate-indicators/climate-change-indicators-atmospheric-concentrations-greenhouse-gases. Published February 23, 2021. Accessed April 8, 2021.

[6]February global temperatures. Earth's CO2 Home Page. https://www.co2.earth/. Accessed April 10, 2022.

[7]Choi, S.; Drese, J. H.; Eisenberger, P. M.; Jones, C. W. Application of amine-tethered solid sorbents for direct CO2 capture from the ambient air. Environ. Sci. Technol. 2011, 45 (6), 2420.

[8]Bollini, Praveen, Nicholas A. Brunelli, Stephanie A Didas, and Christopher W Jones. "Dynamics of CO_2 Adsorption on Amine Adsorbents. 1. Impact of Heat Effects." *I&EC Research Industrial & Chemistry Research*, October 29, 2012.

[9]Stolaroff, J. K.; Keith, D. W.; Lowry, G. V. Carbon dioxide capture from atmospheric air using sodium hydroxide spray. Environ. Sci. Technol. 2008, 42, 2728

[10]Maurer, R. T. Apparent surface diffusion effects for carbon dioxide/air and carbon dioxide/nitrogen mixtures with pelleted zeolite beds. In Adsorption and Ion Exchange with Synthetic Zeolites. Flank, W. H., Ed.; American Chemical Society. 1980, p 73.

[11]Lozinska, Magdalena M., Enzo Mangano, John P. S. Mowat, Ashley M. Shepherd, Russell F.
Howe, Stephen P. Thompson, Julia E. Parker, Stefano Brandani, and Paul A. Wright. "Understanding Carbon Dioxide Adsorption on Univalent Cation Forms of the Flexible Zeolite Rho at Conditions Relevant to Carbon Capture from Flue

Gases." *Journal of the American Chemical Society* 134, no. 42 (November 2012): 17628–42. https://doi.org/10.1021/ja3070864.

[12]Ritter SK. What Can We Do With Carbon Dioxide? C&EN. https://cen.acs.org/articles/85/i18/Carbon-Dioxide.html. Published April 30, 2007. Accessed April 8, 2021.

[13] Stuckert NR, Yang RT. Co2 capture from the atmosphere and simultaneous concentration using zeolites and amine-grafted SBA-15. *Environmental Science & Technology*. 2011;45(23):10257-10264. doi:10.1021/es202647a

[14]Ribeiro RPPL, Grande CA, Rodrigues AE. Activated carbon honeycomb monolith – Zeolite 13x hybrid system to capture CO2 from flue gases employing electric swing adsorption. Chemical Engineering Science. 2013;104:304-318. doi:10.1016/j.ces.2013.09.011

[15]Dutcher B, Fan M, Russell AG. Amine-based CO2 Capture Technology Development from the beginning of 2013—A Review. ACS Applied Materials & Interfaces. 2015;7(4):2137-2148. doi:10.1021/am507465f

[16]Huang Q, Thompson J, Bhatnagar S, et al. Impact of flue gas contaminants on monoethanolamine thermal degradation. Industrial & Engineering Chemistry Research. 2013;53(2):553-563. doi:10.1021/ie403426c

[17]Goldman MJ, Fine NA, Rochelle GT. Kinetics of N-nitrosopiperazine formation from nitrite and piperazine in CO2 Capture. Environmental Science & Technology. 2013;47(7):3528-3534. doi:10.1021/es304640f

[18]Fleming E. Home. SidmartinBio. https://www.sidmartinbio.org/which-is-better-chemcad-or-aspen/. Published May 20, 2019. Accessed April 4, 2022.

[19]A multiscale 3D packed bed reactor. COMSOL. https://www.comsol.com/model/a-multiscale-3d-packed-bed-reactor-17019. Accessed April 4, 2022.

[20]Park, I., & Knaebel, K. S. (1992). Adsorption breakthrough behavior: Unusual effects and possible causes. *AIChE Journal*, *38*(5), 660–670. https://doi.org/10.1002/aic.690380504

[21]Mohan, N., Kannan, G. K., Upendra, S., Subha, R., & Kumar, N. S. (2009). Breakthrough of toluene vapours in granular activated carbon filled packed bed reactor. *Journal of Hazardous Materials*, *168*(2), 777–781. https://doi.org/10.1016/j.jhazmat.2009.02.079

[22]Bonjour, J., Chalfen, J.-B., & Meunier, F. (2002). Temperature Swing Adsorption Process with Indirect Cooling and Heating. *Industrial & Engineering Chemistry Research*, *41*(23), 5802–5811. https://doi.org/10.1021/ie011011j

[23]Sircar, S. (2002). Pressure Swing Adsorption. *Industrial & Engineering Chemistry Research*, *41*(6), 1389–1392. https://doi.org/10.1021/ie0109758

[24]Zhao, R., Zhao, L., Deng, S., Song, C., He, J., Shao, Y., & Li, S. (2017). A comparative study on CO2 capture performance of vacuum-pressure swing adsorption and pressure-temperature swing adsorption based on carbon pump cycle. *Energy*, *137*, 495–509. https://doi.org/10.1016/j.energy.2017.01.158

[25]Cho, S. Y., Yetter, R. A., & Dryer, F. L. (1992). A computer model for one-dimensional mass and energy transport in and around chemically reacting particles, including complex gas-phase chemistry, multicomponent molecular diffusion, surface evaporation, and heterogeneous reaction. *Journal of Computational Physics*, *102*(1), 160–179. https://doi.org/10.1016/S0021-9991(05)80013-0

[26]Van Heest, T., Teich-McGoldrick, S. L., Greathouse, J. A., Allendorf, M. D., & Sholl, D. S. (2012). Identification of Metal–Organic Framework Materials for Adsorption Separation of Rare Gases: Applicability of Ideal Adsorbed Solution Theory (IAST) and Effects of Inaccessible Framework Regions. *The Journal of Physical Chemistry C*, *116*(24), 13183–13195. https://doi.org/10.1021/jp302808j

[27]Wahby, A., Ramos-Fernández, J. M., Martínez-Escandell, M., Sepúlveda-Escribano, A., Silvestre-Albero, J., & Rodríguez-Reinoso, F. (2010). High-Surface-Area Carbon Molecular Sieves for Selective CO2 Adsorption. *ChemSusChem*, *3*(8), 974–981. https://doi.org/10.1002/cssc.201000083

[28]Marczewski, A. W. (2010). Analysis of Kinetic Langmuir Model. Part I: Integrated Kinetic Langmuir Equation (IKL): A New Complete Analytical Solution of the Langmuir Rate Equation. *Langmuir*, *26*(19), 15229–15238. https://doi.org/10.1021/la1010049

[29]Walsh, K., Mayer, S., Rehmann, D., Hofmann, T., & Glas, K. (2020). Equilibrium data and its analysis with the Freundlich model in the adsorption of arsenic(V) on granular ferric hydroxide. *Separation and Purification Technology*, *243*, 116704. https://doi.org/10.1016/j.seppur.2020.116704

[30]Umpleby, R. J., Baxter, S. C., Chen, Y., Shah, R. N., & Shimizu, K. D. (2001). Characterization of Molecularly Imprinted Polymers with the Langmuir−Freundlich Isotherm. *Analytical Chemistry*, *73*(19), 4584–4591. https://doi.org/10.1021/ac0105686

[31]Ruthven, D. M. (Douglas M. *Principles of adsorption and adsorption processes*. (Wiley, 1984).

[32]Zhang, R. & Ritter, J. A. New approximate model for nonlinear adsorption and diffusion in a single particle. *Chem. Eng. Sci.* **52**, 3161–3172 (1997).

[33]Sircar, S. & Hufton, J. R. Why does the linear driving force model for adsorption kinetics work? *Adsorption* **6**, 137–147 (2000).

[34]Buzanowski, M. A. & Yang, R. T. Approximations for intraparticle diffusion rates in cyclic adsorption and desorption. *Chem. Eng. Sci.* **46**, 2589–2598 (1991).

[35] Roy, S., & Moharir, A. (2019). *Modeling the Generic Breakthrough Curve for Adsorption Process*.

[36]Macdonald, I. F., El-Sayed, M. S., Mow, K., & Dullien, F. A. L. (1979). Flow through Porous Media-the Ergun Equation Revisited. *Industrial & Engineering Chemistry Fundamentals*, *18*(3), 199–208. https://doi.org/10.1021/i160071a001

[37]Thompson JA. EVALUATION AND APPLICATION OF NEW NANOPOROUS MATERIALS FOR ACID GAS SEPARATIONS. 2013.

[38]Chapra SC, Canle RP. *Numerical Methods for Engineers*. New York: McGraw-Hill; 2021.

[39]Chu KH. Breakthrough curve analysis by simplistic models of fixed bed adsorption: In defense of the Century-old Bohart-Adams model. *Chemical Engineering Journal*. 2020;380:122513. doi:10.1016/j.cej.2019.122513

[40]*scipy.optimize.curve_fit—SciPy v1.8.0 Manual*. (n.d.). Retrieved April 5, 2022, from https://docs.scipy.org/doc/scipy/reference/generated/scipy.optimize.curve_fit.html

[41]Xu M, Deng S. Carbon Capture from Air Project. 2020

[42]Bonelli XB. Adsorptive CO¬2 Capture from Ambient Air by Zeolites. 2021

[43]Ciha T. Prediction of Multicomponent Gas Adsorption Equilibrium for Direct Air Capture Using Ideal Adsorbed Solution Theory. 2022.

APPENDIX A

MODEL I AND MODEL II CODE

```
################################
# Breakthrough Model Simulation (Model 2)
# Author: Xavier Bonelli
################################

import numpy as np
import matplotlib.pyplot as plt
import pandas as pd

# Isotherm Parameters
# Component 1: CO2
# Component 2: N2
# Component 3: H2O
components = 3 #Number of components
qmax = np.zeros(components, dtype=float) #Saturation loading of each
component
qmax[0] = 101.588762917714 #mol/kg
qmax[1] = 63.6585 #mol/kg
qmax[2] = 0 #mol/kg
bi = np.zeros(components, dtype=float)
bi[0] = 0.2958340160420933 #kPa^-1  #Langmuir constant
bi[1] = 0.0014282121524645475 #kPa^-1
bi[2] = 0 #kPa^-1
RHO = 0.241 #kg/L, Framework density
#=============================================================================
#
#Sample Data Import
data = pd.read_csv("sampledata1.csv")
ppm = data.pop("PPM")
time = data.pop("Time")
time_list = time.to_numpy()
C0 = 415
adjust = ppm/C0
ppm_list = adjust.to_numpy()
#=============================================================================
#
#Thermodynamic data
Temp = 273.15 + 25 # Input temperature in degrees Celsius, K
R = 8.314 # Ideal gas constant, kPa*L/mol/K
p0 = 100 # Starting total pressure, kPa
y0 = np.zeros(components, dtype=float) # Starting mole fraction
y0[0] = 0.0004 #Component 1
y0[1] = 0.9996 #Component 2
y0[2] = 0.5 #Component 3,
```

```
eps = 0.21 #Bed voidage
bed_diameter = 0.0127; # meters
bed_area = (bed_diameter/2)**2*np.pi #cross sectional area of the bed
flow_rate = 0.00333333333333 # meters^3 per second
u0 = flow_rate/bed_area #Velocity, m/sec
bed_length = 0.56 #meters
#========================================================================#
#Discretization and initialization
delz = 0.01 #Discretized bed length, bed is normalized to 0-1
zmax = 1.0 #Dimensionless bed length
m = int(zmax/delz) #Number of points
z = np.zeros([1,m+1], float) #Zeroed z matrix
delt = 100. #Discretized time scale, time is normalized to velocity and
bed
tmax = 450000. #Max breakthrough time, dimensionless time
n = int(tmax/delt) #Number of points
t = np.zeros([n+1,1], float) #Zeroed t matrix
p1 = np.zeros([n+1,m+1], float) #Matrix for pressure 1
p2 = np.zeros([n+1,m+1], float) #Matrix for pressure 2
p3 = np.zeros([n+1,m+1], float) #Matrix for pressure 3
py1 = np.zeros([n+1,m+1], float) #Matrix for pressure 1
py2 = np.zeros([n+1,m+1], float) #Matrix for pressure 2
py3 = np.zeros([n+1,m+1], float) #Matrix for pressure 3
p3 = np.zeros([n+1,m+1], float) #Matrix for pressure 3
p1store = np.zeros([1,m+1], float) #Storage matrix
p2store = np.zeros([1,m+1], float) #Storage matrix
ustore = np.zeros([1,m+1], float) #Storage matrix
y1 = np.zeros([n+1,m+1], float) #Matrix for mole fraction 1
y2 = np.zeros([n+1,m+1], float) #Matrix for mole fraction 2
y3 = np.zeros([n+1,m+1], float) #Matrix for mole fraction 3
u = np.zeros([n+1,m+1], float) #Matrix for superficial velocity
u2= u
q1 = np.zeros([n+1,m+1], float) #Matrix for adsorbed gas 1
q2 = np.zeros([n+1,m+1], float) #Matrix for adsorbed gas 2
q3 = np.zeros([n+1,m+1], float) #Matrix for adsorbed gas 3
ustore = np.zeros([1,m+1], float)
#========================================================================#
#Initial Conditions
for i in range(0 , m + 1):
    p1[0,i] = 0
    p2[0,i] = 0
    p3[0,i] = 0
    py1[0,i] = 0
    py2[0,i] = 0
```

```
    py3[0,i] = 0
    y1[0,i] = 0
    y2[0,i] = 0
    y3[0,i] = 0
    u[0,i] = 0
    u2[0,i] = 0
#=========================================================================#
#Boundary Conditions
p1_comp = y0[0]*p0
p2_comp = y0[1]*p0
p3_comp = y0[2]*p0
#for loop to  replace first entry in every row with the initial pressure
times the component fraction
for j in range (1, n+1):
    p1[j,0] = p1_comp
    p2[j,0] = p2_comp
    p3[j,0] = p3_comp
    py1[j,0] = p1_comp
    py2[j,0] = p2_comp
    py3[j,0] = p3_comp
    y1[j,0] = y0[0]
    y2[j,0] = y0[1]
    y3[j,0] = y0[2]
    u[j,0] = 1

for i in range(0,m):
    z[0,i+1] = z[0,i] + delz
for i in range(0, n):
    t[i+1,0] = t[i,0] + delt
#=========================================================================
#
#PDE Solver
for j in range (1, m+1):
    for i in range (0, n):
        p0=100
        dq1dy = qmax[0]*bi[0]*p0*(1+bi[1]*p0)/(1+y1[i,j]*p0*(bi[0]-
bi[1])+bi[1]*p0) #Langmuir isotherm
        dq2dy = -qmax[1]*bi[1]*p0*(1+bi[0]*p0)/(1+y1[i,j]*p0*(bi[0]-
bi[1])+bi[1]*p0) #Langmuir isotherm
        func1 = 1+(1-eps)/eps*RHO*R*Temp/p0*((1-
y1[i,j])*dq1dy+y1[i,j]*dq2dy) #mass balance for componet 1
        func2 = -(1-eps)/eps**2*RHO*R*Temp/p0*(dq1dy+dq2dy) #mass balance
for component 2
```

```
        u11 = u[i,j-1] + delz*func2*u[i,j-1]*eps/func1*(y1[i,j]-y1[i,j-
1])/delz
        y11 = y1[i,j]-delt*u11*eps/func1*(y1[i,j]-y1[i,j-1])/delz
        y22 = (1-y11)
        yt = y11 + y22
        if u11 == 0:
                p0 = 0
        else:
            p0 = 100

        y1[i+1,j] = y11
        y2[i+1,j] = y22
        u[i,j] = u11
        py1[i+1,j] = y11*p0
        py2[i+1,j] = y22*p0
        if j == m:
            if y11 <= 0.02:
                tbreak = t[i+1]
                p1store = py1[i+1,:]
                p2store = py2[i+1,:]
                ustore = (u[i,:])-1
            if y11/y0[0] <= 0.5:
                tstoich = t[i+1,0]



yval = py1[:,m]
yval1 = yval/p0
yval2 = yval1/y0[0]
t_fix = ((t*bed_length*eps/u0)/60)
plt.plot(t_fix,yval2, color = "blue", label = "Modeled Data")
plt.xlabel("Time (min)")
plt.ylabel("Concentration (C/C0)")
plt.scatter(time_list,ppm_list, color = "red", marker = "x", label =
"Experimental Data")
plt.legend()
plt.show()
```

```
################################################
# Empirical Breakthrough Data Fitting Model
# Author: Xavier Bonelli
#Package Imports
################################################
from tkinter import Y
import pandas as pd
import numpy as np
import matplotlib.pyplot as plt
from scipy.optimize import curve_fit
import PySimpleGUI as sg

#General Breakthrough shape fitting formula for creating a Sigmoid
def breakfit (t,a,b):
        return 1 / ( 1 + np.exp (a - t * b))

#Imports sample data and splits it into time vs concentration
dataframe = input("Sample Data File Name: ")
data = pd.read_csv(dataframe)
ppm = data.pop("PPM")
time = data.pop("Time")
time_list = time.to_numpy()

#Initial Concentration
C0 = float(input("Inlet Concentration: "))
adjust = ppm/C0
ppm_list = adjust.to_numpy()
A = float(input("Initial Guess for a: "))
B = float(input("Initial Guess for b: "))
#Least Squared Regression + Fsolve to find model constants a and b
popt, pcov = curve_fit(breakfit, time_list, ppm_list, [A,B],
bounds=(0.00000001,np.inf)) \
    #function, x values, y values, initial guess, range of possible values

#prints the model obtained constants
print(f'a = {popt[0]}')
print(f'b = {popt[1]}')

#initialization matrix of solutions
solutions = []

#runs time values through the model to be fit
for i in time_list:
    point = breakfit(i,popt[0],popt[1])
```

```
    solutions.append(point)

#plots the results
plt.scatter(time_list,ppm_list, color = "red", marker = "x", \
    label = "Experimental Data")
plt.plot(time_list, solutions, color = "blue", label = "Modeled Data")
plt.xlabel("Time (Minutes)")
plt.ylabel("C/C0")
plt.legend()
plt.show
```